ETH
Eidgenössische Technische Hochschule Zürich
Swiss Federal Institute of Technology Zurich

Seminar for Applied Mathematics SAM

Edge and Corner Detection with Parabolic Dictionaries

P. Grohs and Z. Kereta

Research Report No. 2016-40
September 2016

Seminar für Angewandte Mathematik
Eidgenössische Technische Hochschule
CH-8092 Zürich
Switzerland

Edge and Corner Detection with Parabolic Dictionaries

Philipp Grohs*[1] and Željko Kereta†[1]

[1]*ETH-Zürich.*

Abstract

Last decade saw the creation of a number of directional representation dictionaries that desire to address the weaknesses of the classical wavelet transform that arise due to its limited capacity for the analysis of edge-like features of two-dimensional signals. Salient features of these dictionaries are directional selectivity and anisotropic treatment of the axes, achieved through the parabolic scaling law. In this paper we will examine the adequacy of such dictionaries for the detection of edge- and corner-like features of 2D regions through a comprehensive framework for directional parabolic dictionaries, called the continuous parabolic molecules. This work builds on a family of earlier studies and aims to give a broader perspective through the level of generality.

1 Introduction

The problem of detecting edges and other geometrical discontinuities of a function is a topic of fundamental interest for many problems in image analysis, numerical solutions of partial differential equations and approximation theory. For example, many existing techniques of digital medical imaging, such as magnetic resonance imaging, encode a signal by digitising it with the Fourier transform. The image is then obtained by one of many methods of Fourier reconstruction [1, 2], which ought to take into account that due to various imperfections that exist in the signal acquisition process, the data might be noisy and incomplete. In many cases, to reach a useful diagnosis it is sufficient to know only the shapes that outline and separate the areas of interest, rather than the fine details of the image. Therefore, robust methods of edge detection are vital.

Due to its importance in a host of applications, this topic has naturally received a lot of attention over the years. The majority of contemporary high-dimensional edge detection methods are essentially one-dimensional, that is, they rely on the computation of the singular support of a given function through an application of one-dimensional detection schemes in each coordinate direction. This is due to the fact that singular support of a distribution consists of points ξ, where $\hat{f}(\xi)$ does not decay rapidly as $\|\xi\| \to \infty$. Therefore, we can say that the information regarding the discontinuities of an image is encoded in its high-frequency content, which can be extracted with high-pass filters [1, 3].

Let us look at a simple example. Assume that the input image can be modelled as the indicator function of the unit ball, $f(\mathbf{x}) = \chi_{\mathcal{B}_0(1)}(\mathbf{x})$. The singular support of f, and the boundary of the image, is then the unit sphere $\{\mathbf{x} : \|\mathbf{x}\| = 1\}$. In order to recover the boundary curve, the standard approach would consist of two steps: a computation of

*Email: philipp.grohs@sam.math.ethz.ch

†Email: zeljko.kereta@math.ethz.ch

the points that lie on the boundary and an application of the algorithm that connects the computed points into the desired boundary curve.

The reconstruction of the original curve from the computed points of discontinuity is mired with many practical issues. For example, the set of computed points could be inundated with spurious information if the initial image contains noise, which results in a poor reconstruction. Furthermore, assuming the original image consists of two close by closed curves it might be exceedingly hard to tell the two boundaries apart and associate the points to the correct boundary curve.

We can try to rectify, or at the very least improve, this predicament by using additional information provided by the geometry of the underlying image. The type of information that would be apposite in the context of edges are the directions of the normals at points on the boundary. In terms of microlocal analysis, this would equate to computing the wavefront set of the image, instead of the singular support, since it simultaneously uncovers the points on the boundary and the respective normals. For example, the wavefront set of the unit ball is given as

$$\mathrm{WF}(\chi_{\mathcal{B}_0(\mathbf{1})}) = \{(\theta, (\cos(\theta), \sin(\theta))) : \theta \in [0, 2\pi)\}.$$

Knowing both the locations and the directions of the points of discontinuity would help mitigate the issues that arise in practical applications. Firstly, it is highly unlikely that the directions of normals of spurious points would be consistent with the directions of normals of the points on the actual boundary curve. Hence, this additional geometrical datum can be used to essentially denoise the signal and consequently dispose of any spurious data before we proceed with the reconstruction. Furthermore, the normals of points that lie on the same part of the boundary curve will not deviate too much, thus separating disjoint boundary curves and properly associating each point to its respective part of the boundary will be easier to conduct.

1.1 Generalised Parabolic Dictionaries

Recent years saw the creation of a new generation of dictionaries that try to address the limititations prevalent in classical transforms such as the wavelet analysis. The inherent flaw of classical transforms lies in the fact that they are not adapted for addressing the tasks needed for the analysis of multi-variate signals [4], which is often attributed to their inability to resolve directional features. This led to the development of curvelets [5], shearlets [6], contourlets [7], and other transforms, all of which infuse their architectures with the parabolic scaling law width $\sim$ height^2 and directional sensitivity. Whereas these dictionaries are fundamentally similar, the specifics of how are parabolic dilations of the variables and the reorientations of the generators executed can be vastly different. Nevertheless, the adherence to anistropic directional dictionaries has over the years proved to be useful for many practical (astronomical [8] and seismical [9] imaging, denoising [10], etc.) and theoretical topics (analysis of hyperbolic differential equations [11]).

On account of the similarity in approximation properties and needless repetitions of ultimately bespoke proofs, a framework of parabolic molecules was recently established [12, 13]. Parabolic molecules attempt to be broad enough to encompass the existing parabolic directional dictionaries, and yet specific enough to answer questions of interest.

The adequacy of parabolic directional dictionaries for topics in microlocal analysis has been long established. For example, Candés and Donoho [14], and Kutyniok and Labet [15] showed that the wavefront set of a distribution can be revealed through the decay of the frame coefficients with respect to second generation curvelets and classical, band-limited. shearlets. These, and other select results in microlocal analysis have later been extended to all admissible parabolic molecules [13]. By the preceding argumentation, this feature of parabolic dictionaries is clearly a valuable asset for edge detection. At the heart

of these investigations lies the investigation of rates of decay of frame coefficients with respect to the dilation parameter. For example, the seminal work on second generation curvelets [5] includes a brief investigation of the singularity features of sets in $\mathbb{R}^2$, though the relevant analysis is restricted to polygons and similar objects. The same type of analysis was later performed for band-limited shearlets [15], and then extended to more general sets [16]. A related study was recently conducted for specific constructions of compactly supported shearlets in [17]. On the other hand, Greengard and Stucchio [3] constructed a family of high-pass filters, whose relationship between angle and radial filters satisfy the parabolic scaling law, in order to detect edges of images ,though the focus of the work is somewhat different.

Our goal is to extend and generalise these considerations in the framework of (continuous) parabolic molecules. The methods we shall develop are somewhat of an amalgam of the ideas from [5], [15] and [16], while the discussion in Section 5 was in large part motivated by [18]. The primary contribution of our work lies in the level of generality. In other words, our results on corner and edge detection hold for parabolic dictionaries that satisfy some rather mild assumptions. Most importantly, we pose no assumptions on how are those families constructed (be it in the frequency or in the space domain) nor do we assume anything about their supports. Consequently, the results obtained herein can be applied to general parabolic dictionaries.

Let us summarise our results. We distinguish between edge and corner points. When $\mathbf{p} \in \partial\Omega$ is (just) an edge point of Ω we will show that if a molecule m_λ is not orthogonal to $\partial\Omega$ at $\mathbf{p}$ then we have arbitrarily fast decay $\langle \chi_\Omega, m_\lambda \rangle \lesssim a^N$, whereas, when m_λ is orthogonal to $\partial\Omega$ at $\mathbf{p}$ the decay is slow, $\langle \chi_\Omega, m_\lambda \rangle \lesssim a^{3/4}$. The corner points on the other hand demand considerably more attention and we will need to use an approximation argument to address general closed curves Ω. In the end, we will show that for a corner point $\mathbf{p} \in \partial\Omega$ we again have $\langle \chi_\Omega, m_\lambda \rangle \lesssim a^{3/4}$, if m_λ is orthogonal to $\partial\Omega$ at $\mathbf{p}$, and otherwise $\langle \chi_\Omega, m_\lambda \rangle \lesssim a^{5/4}$ (Theorem 4.11). Therefore, whereas the frame coefficients for edge points have one direction of slow decay, and all other directions give fast decay, in case of corner points the decay will be slow for the two directions that correspond to the normals, and it will be marginally faster for all other directions.

The drawbacks that come when the framework is as general as it is here are rather obvious. The crux of our results is that they are of only qualitative nature (though a more detailed analysis could yield better quantitative estimates), and we can only produce upper bounds on frame coefficients. The presently available research, for example [17] and [16], seems to suggest that it would be reasonable to expect that the upper bounds on the frame coefficients are unattainable at this level of generality, since the existing proofs depend delicately on the specifics of each construction.

1.2 Contents

We will begin in Section 2, where we will define continuous parabolic molecules. In Section 3 where we will briefly assess the edge points and Section 4 will be devoted to the analysis of corner points. The analysis of angular wedges in Section 4.1 will be the starting point for the analysis of general sets through an approximation procedure. In Section 4.5 we will describe and extended the results of Section 4.1 to general sets. Section 5 will be devoted to the study of decay rates of frame coefficients when the indicator function of the set in question is multiplied by a smooth function. The purpose of Section 6 is to ask (and answer) the question of what would change if we chose a different scaling law. We will finish off in Sections 7 and 8 with a simple numerical study and a brief discussion of further directions that could be pursued.

1.3 Notation

Throughout this paper we will use $\mathbf{p}$ to denote the arbitrary point of interest in $\mathbb{R}^2$. When we say that an angle θ_λ, is normal or orthogonal to a bounded open set $\Omega \subseteq \mathbb{R}^2$, or to its boundary $\partial\Omega$, at a point $\mathbf{p}$, or to some angle, what me mean is that $\cos(\eta + \theta_\lambda) = 0$, where η is the angle of the normal at $\mathbf{p} \in \partial\Omega$. Analogously, we will say that a molecule m_λ, with $\lambda = (a_\lambda, \theta_\lambda, \mathbf{p})$, is orthogonal to Ω, or to $\partial\Omega$, if $\mathbf{p} \in \partial\Omega$ and θ_λ is normal to $\partial\Omega$ at $\mathbf{p}$.

We will use $L^p(\mathbb{R}^d)$ to denote the Lebesgue space of functions associated with the norm $\|\cdot\|_p$. The Fourier transform of an $L^1(\mathbb{R}^d)$ function f is defined as

$$\widehat{f}(\boldsymbol{\xi}) = \int_{\mathbb{R}^d} f(\mathbf{x}) e^{-2\pi\imath \mathbf{x}\cdot\boldsymbol{\xi}} d\mathbf{x}.$$

This definition can be extended to tempered distributions using standard density arguments.

With $\langle\cdot,\cdot\rangle$ we will denote either the dot product of two functions, or the action of a distribution on a given function. On the other hand, when there is only one argument then $\langle\cdot\rangle$ is defined as $\langle x\rangle = (1+x^2)^{1/2}$. Throughout this paper we will work in $\mathbb{R}^2$, with a spatial variable $\mathbf{x}$, while $\boldsymbol{\xi}$ will be reserved to variables in the frequency space. The notation $A \lesssim B$ will be used to indicate that $A \leqslant CB$ where C is a constant that does not depend on neither A nor B.

2 Continuous Parabolic Molecules

We begin by introducing the basic definitions and ideas regarding continuous parabolic molecules (herein CPMs). Define the parameter space as

$$\mathbb{P} = \mathbb{R} \times [0, 2\pi) \times \mathbb{R}^2,$$

where a point $(a, \theta, \mathbf{b}) \in \mathbb{P}$ describes a scale a, an orientation θ, and a location $\mathbf{b}$.

Let $R_\theta = \begin{pmatrix} \cos(\theta) & -\sin(\theta) \\ \sin(\theta) & \cos(\theta) \end{pmatrix}$ be the rotation matrix through the angle θ, and let $D_a = \operatorname{diag}(a, a^{1/2})$ be the (parabolic) dilation matrix, with $a \in \mathbb{R}^+$.

Definition 2.1. A family of functions $\{m_\lambda : \lambda \in \Lambda\}$ is called a family of *continuous parabolic molecules* of order (R, M, N_1, N_2) if it can be written as

$$m_\lambda(\mathbf{b}) = a_\lambda^{-3/4} \varphi^{(\lambda)} \left(D_{1/a_\lambda} R_{\theta_\lambda} (\mathbf{b} - \mathbf{b}_\lambda) \right),$$

where $(a_\lambda, \theta_\lambda, \mathbf{b}_\lambda) = \Phi(\lambda) \in \mathbb{P}$ and $\varphi^{(\lambda)}$ satisfies

$$|\partial^\beta \widehat{\varphi}^{(\lambda)}(\boldsymbol{\xi})| \lesssim \min\left(1, a_\lambda + |\xi_1| + a_\lambda^{1/2}|\xi_2|\right)^M \langle \|\boldsymbol{\xi}\| \rangle^{-N_1} \langle \xi_2 \rangle^{-N_2} \tag{1}$$

for all multi-indices $|\beta| \leqslant R$. The implicit constants are uniform over λ.

The map $\Phi : \Lambda \to \mathbb{P}$ is called a parametrisation. Since dictionaries abide by different architectures, they might for example have different approaches to treating orientations, we use the parametrisation mapping to say how do their native indices correspond to scaling, orientation and location parameters. To simplify the notation, we will identify λ with $(a_\lambda, \theta_\lambda, \mathbf{b}_\lambda)$, instead of writing $(a_\lambda, \theta_\lambda, \mathbf{b}_\lambda) = \Phi(\lambda)$, which should not lead to confusion. Furthermore, in most of the proofs we will also drop the λ subscripts for the sake of less cumbersome notation. There are further notions that are required for a full description of the framework (e.g. admissibility of parametrisations), but they are not relevant for the present discussion and we refer to [12, 13] for more details.

Definition 2.1 suggests a number of properties: a (somewhat biased) directional decay as the coordinates tend to infinity, M almost vanishing moments, and frequency localisation with respect to the dilation parameter a_λ. Furthermore, $R \in \mathbb{N}$ describes the spatial localisation of the molecule m_λ while N_1 and N_2 correspond to its smoothness. The law of parabolic scaling is propagated through the dilation matrix D_a. As we will see in Section 6, when it comes to the detection of edges and corner points, we do not need to adhere to the parabolic scaling. there are many other viable choices as long as some directional bias is present. This can be achieved by replacing $a^{1/2}$ in the definition of D_a with a^α, for $\alpha \in (0,1)$.

The foremost examples of families of continuous parabolic molecules are second generation curvelets and cone-adapted shearlets and one can show that they are both CPMs of arbitrary order.

Since we will mostly be working in the Fourier domain, let us note that the Fourier transform of m_λ is given as

$$\widehat{m}_\lambda(\xi) = a_\lambda^{3/4} e^{-2\pi\imath \mathbf{b}\cdot\xi} \widehat{\varphi}^{(\lambda)}\left(D_{a_\lambda} R_{\theta_\lambda} \xi\right).$$

The fundamental property of CPMs is *almost orthogonality*. Essentially, this means that the inter-Gramian of two CPM families exhibits strong off-diagonal decay with respect to the pseudo-distance function

$$w(\lambda,\nu) = \frac{a_M}{a_m}\left(1 + a_M^{-1} d(\lambda,\nu)\right),$$

where

$$\begin{aligned} a_m &= \min(a_\lambda, a_\nu), \\ a_M &= \max(a_\lambda, a_\nu), \\ d(\lambda,\nu) &= |\theta_\lambda - \theta_\nu|^2 + |\mathbf{b}_\lambda - \mathbf{b}_\nu|^2 + |\langle \mathbf{e}_\lambda, \mathbf{b}_\lambda - \mathbf{b}_\nu\rangle|, \\ \mathbf{e}_\lambda &= (\cos(\theta_\lambda), \sin(\theta_\lambda))^\top, \end{aligned}$$

which was motivated by the work of Smith [19], Candés and Demanet [11], and Grohs and Kutyniok [12].

Theorem 2.1. *Let $\Gamma = \{m_\lambda : \lambda \in \Lambda^\Gamma\}$ and $\Sigma = \{n_\nu : \nu \in \Lambda^\Sigma\}$ be two families of continuous parabolic molecules, both of order (R, M, N_1, N_2). Then*

$$|\langle m_\lambda, n_\nu\rangle| \leqslant w(\lambda,\nu)^{-N}$$

holds for every $N \in \mathbb{N}$ such that

$$R \geqslant 2N, \quad M > 3N - \frac{5}{4}, \quad N_1 \geqslant N + \frac{3}{4}, \quad N_2 \geqslant 2N.$$

Almost orthogonality of CPMs can be used to infer that some results in microlocal analysis, such as the resolution of the wavefront set or the microlocal Sobolev regularity, are universal for all good-enough families of CPMs.

2.1 Wavefront Set

Let us now formalise the notion of the wavefront set. We say that a set $\mathcal{C}$ is a cone if for every $\xi \in \mathcal{C}$ and every $t > 0$ we have $t\xi \in \mathcal{C}$.

Definition 2.2. The *wavefront set* of a distribution f, denoted $WF(f)$, is the complement of the set of all points $(\theta_0, \mathbf{b}_0)$ such that there exists a smooth window function $\phi \in C_0^\infty$, $\phi(\mathbf{b}_0) \neq 0$ and an open cone $\mathcal{C}$ such that $\theta_0 \in \mathcal{C}$, with the property that for all $N \in \mathbb{N}$

$$|\widehat{\phi f}(\xi)| \leqslant C_N(1 + \|\xi\|)^{-N}, \text{ for all } \xi \in \mathcal{C}. \tag{2}$$

As we already mentioned, one of the important features of curvelets and shearlets is their ability to uncover the wavefront set of a distribution as the complement of the set of points where the corresponding frame coefficients decay rapidly. To be more specific, if we denote by $\gamma_{a\,\theta\,\mathbf{b}}$ the second generation curvelets [5], then $\mathrm{WF}(f)$ is the complement of the set of points $(\theta_0, \mathbf{b}_0)$ such that

$$\langle f, \gamma_{a\,\theta\,\mathbf{b}} \rangle \lesssim a^N, \text{for all } N \in \mathbb{N}, \text{ as } a \to 0,$$

for $(\theta, \mathbf{b})$ are in some open neighbourhood of $(\theta_0, \mathbf{b}_0)$. In [13] it was shown that this result is indeed universal for all families of CPMs that satisfy mild conditions, which we will not go into for the sake of brevity.

Theorem 2.2. *Let $\Sigma = \{n_\nu : \nu \in \Lambda_\Sigma\}$ be a family of continuous parabolic molecules of order (R, M, N_1, N_2), and $(\Psi_\Sigma, \Lambda_\Sigma)$ its parametrisation. The wavefront set of f is the complement of*

$$R_\Sigma = \Bigg\{ (\theta_0, \mathbf{b}_0) : \textit{for all } k \in \mathbb{N} \textit{ we have } |\langle f, n_{\Psi_\Sigma^{-1}(a,\theta,\mathbf{b})} \rangle| = \mathcal{O}(a^k) \textit{ as } a \to 0, \\ \textit{for some neighbourhood } \mathcal{N} \textit{ of } (\theta_0, \mathbf{b}_0) \Bigg\}. \quad (3)$$

3 Detection of Edges

Consider a bounded, open set $\Omega \subseteq \mathbb{R}^2$ with a continuous and piecewise-smooth boundary $\partial\Omega$ and let χ_Ω denote its indicator function. As we mentioned earlier, it can be shown that the wavefront set of χ_Ω is given by

$$\mathrm{WF}(\chi_\Omega) = \{(\theta, \mathbf{x}) : \mathbf{x} \in \partial\Omega, \theta \text{ normal to } \partial\Omega \text{ at } \mathbf{x}\}. \quad (4)$$

The proof of (4) can be found in [20]. On the other hand, Theorem 2.2 states that the wavefront set is the complement of the set of angle-location pairs for which the frame coefficients with respect to a family of CPMs decay rapidly as the dilation parameter goes to zero. Let us summarise this in a theorem.

Theorem 3.1. *Let $\Omega \subseteq \mathbb{R}^2$ be a bounded and open set with continuous and piecewise-smooth boundary $\partial\Omega$, and let $\Gamma = \{m_\lambda : \lambda \in \Lambda_\Gamma\}$ be a family of continuous parabolic molecules that satisfy the assumptions of Theorem 2.2. Then if a point $\mathbf{p} \in \mathbb{R}^2$ does not lie on the boundary curve $\partial\Omega$ and the angle $\theta_\lambda \in [0, 2\pi)$ is arbitrary, we have*

$$\langle \chi_\Omega, m_\lambda \rangle \lesssim a_\lambda^N, \quad \textit{for all } N \in \mathbb{N},$$

for $\lambda = (a_\lambda, \theta_\lambda, \mathbf{p})$. Otherwise, if $\mathbf{p}$ lies on the boundary curve $\partial\Omega$, and $\partial\Omega$ is C^∞ in the neighbourhood of $\mathbf{p}$, then taking θ_λ which is normal to $\partial\Omega$ at $\mathbf{p}$, we again have

$$\langle \chi_\Omega, m_\lambda \rangle \lesssim a_\lambda^N, \quad \textit{for all } N \in \mathbb{N}.$$

Proof. The statement follows directly by comparing (4) with Theorem 2.2. □

This result is of only qualitative nature, that is to say, the dependence of the decay rates on the order of the given CPM family and on the smoothness of the boundary in the vicinity of $\mathbf{p}$ could be made more explicit, but such considerations are not pertinent for the present discussion.

This still leaves a couple of unanswered questions. The first question concerns the decay rates of the frame coefficients $\langle \chi_\Omega, m_\lambda \rangle$ when $\mathbf{p}$ lies on the boundary of Ω and the angle θ_λ is normal to $\partial\Omega$ at $\mathbf{p}$. Studies conducted in [5, 16, 17] indicate that the answer is exactly $a_\lambda^{3/4}$. We will not focus on this question since we cannot obtain lower bounds

within this framework, whereas the upper bound can be derived through a very simple argument using the fact that χ_Ω is in L^∞ by

$$|\langle \chi_\Omega, m_\lambda \rangle| \leqslant a_\lambda^{3/4} \int_{\mathbb{R}^2} |\varphi^{(\lambda)}(\mathbf{x})| d\mathbf{x} \lesssim a_\lambda^{3/4}. \tag{5}$$

This is up to a multiplicative constant the same as what can be reached through substantially more delicate means, such as in [16, 17]. Therefore, we will not pursue this question any further.

The second interesting question concerns the points were the boundary is not smooth. This is the question we will focus on in the rest of this chapter. These are the points where the boundary curve is continuous but the derivative is not uniquely defined, or in other words, the tangents from the left and from the right at those points on the boundary are not aligned.

4 Corner Points

4.1 Wedges

The first order of business is to define what is a corner point of a set $\Omega \subseteq \mathbb{R}^2$. We will follow the definitions from [16].

Definition 4.1. Let $\Omega \subseteq \mathbb{R}^2$ be a bounded and open set with continuous and piecewise-smooth boundary that has non-vanishing and bounded curvature. Denote by $\alpha_\Omega : [0,1] \to \mathbb{R}^2$ the parametrisation of the boundary $\partial\Omega$ (which we may assume to be an arc-length parametrisation). We say that a point $\mathbf{p} \in \partial\Omega$ is a *corner point* of Ω if $\alpha'_\Omega(t_0^+) \neq \pm\alpha'_\Omega(t_0^-)$, where $\mathbf{p} = \alpha_\Omega(t_0)$.

The condition $\alpha'_\Omega(t_0^+) = \pm\alpha'_\Omega(t_0^-)$ is also excludes the sets whose boundary is Möbius-like. That is, when following the path of the normal all the way back to the starting point we end up on the same line but facing the opposite direction. This can happen for example if the number of crossings in a curve is odd, or equivalently, if the winding number of a point in the interior of the curve is even, thus reversing the orientation of the normals.

The first step in computing the decay rates of the frame coefficients is showing that they are a local property.

Lemma 4.1. *Consider two tempered distributions f_1 and f_2 such that $f_1 = f_2$ in an open neighbourhood of $\mathbf{p} \in \mathbb{R}^2$ and let $\Gamma = \{m_\lambda : \lambda \in \Lambda_\Gamma\}$ be a family of continuous parabolic molecules of order (R, M, N_1, N_2) such that $N_1 > 4$. Then for $\lambda = (a_\lambda, \theta_\lambda, \mathbf{p})$ and $\rho \in \mathbb{N}$, we have, provided $R \geqslant 2\rho$,*

$$\langle f_1, m_\lambda \rangle \sim a^\rho \text{ if and only if } \langle f_2, m_\lambda \rangle \sim a^\rho, \text{ as } a \to 0.$$

Proof. Let us first assume that f_1 and f_2 are bounded compactly supported functions. This can then be extended to tempered distributions through standard arguments. We can assume without loss of generality that f_1 and f_2 coincide on a ball $\mathcal{B}_\epsilon(\mathbf{p})$. We have

$$\begin{aligned} |\langle f_1, m_\lambda \rangle - \langle f_2, m_\lambda \rangle| &= \left| \int_{\mathbb{R}^2} \overline{m_\lambda}(\mathbf{x})(f_1 - f_2)(\mathbf{x}) d\mathbf{x} \right| \\ &\leqslant \|f_1 - f_2\|_{L^\infty(\mathcal{B}^c(\mathbf{p}))} \int_{\mathcal{B}_\epsilon^c(\mathbf{p})} |m_\lambda(\mathbf{x})| d\mathbf{x}. \end{aligned}$$

We will omit the λ indices from now on. Writing $M = D_{1/a} R_\theta$ we have

$$m(\mathbf{x}) = a^{-3/4} \varphi(M(\mathbf{x} - \mathbf{p})).$$

Through standard methods we get

$$\varphi(\mathbf{x}) = \int_{\mathbb{R}^2} \hat{\varphi}(\xi) e^{2\pi\imath \mathbf{x}\cdot\xi} d\xi = (-1)^k (2\pi\|\mathbf{x}\|)^{-2k} \int_{\mathbb{R}^2} \Delta^k \hat{\varphi}(\xi) e^{2\pi\imath \mathbf{x}\cdot\xi} d\xi.$$

Using Jensen's inequality we then have

$$|\varphi(\mathbf{x})| \leqslant C_k 2^{k-1} \left(1 + \|\mathbf{x}\|^2\right)^k = \tilde{C}_k \langle \|\mathbf{x}\| \rangle^{-2k},$$

holds for all $k \in \mathbb{N}$ for which $\Delta^k \hat{\varphi}$ exists and such that

$$\int_{\mathbb{R}^2} |\hat{\varphi}(\xi)| d\xi < \infty, \quad \text{and} \quad \int_{\mathbb{R}^2} |\Delta^k \hat{\varphi}(\xi)| d\xi < \infty. \tag{6}$$

Due to conditions (1), the terms in (6) hold as long as the CPM family Γ is of order (R, M, N_1, N_2), where $R \geqslant 2k$ and $N_1 \geqslant 4$. Therefore, we have

$$|\varphi(M(\mathbf{x} - \mathbf{p}))| \leqslant C_k 2^{k-1} \langle \|M(\mathbf{x} - \mathbf{p})\| \rangle^{-2k}. \tag{7}$$

Now, since $\|M\mathbf{u}\| \geqslant a^{-1/2}\|\mathbf{u}\|$, it follows

$$\int_{\mathcal{B}_\epsilon^c(\mathbf{p})} |m(\mathbf{x})| d\mathbf{x} \leqslant C_k a^k \int_{\mathcal{B}_\epsilon^c(\mathbf{p})} (a + \|\mathbf{u}\|^2)^{-k} d\mathbf{u} \leqslant C_{k,\epsilon} a^k,$$

as long as $k > 1$. Therefore, the conclusion follows. □

From this point forward we will assume that any family of CPMs satisfies the conditions of Lemma 4.1.

Let us now describe the strategy that we will argue in the remainder of the paper. We will begin by considering angular wedges (such as in Figure 4.1), which are prototypical examples of sets in $\mathbb{R}^2$ with corner points. A simple argument using the localisation Lemma 4.1 then allows for the corner detection in polygons. In order to address more general sets we will use an approximation argument in which the boundary of a given set Ω will, in the vicinity of a corner point, be approximated with straight lines determined by the two tangents that define the corner point. We will show that the information regarding the decay rates is preserved throughout this process.

To begin, let $\mathcal{W}_{\eta_1,\eta_2} \subseteq \mathbb{R}^2$ denote an angular wedge centred at the origin, where $0 < \eta_1 < \eta_2 < 2\pi$ and $\eta_2 - \eta_1 \neq \pi$, defined by

$$\mathcal{W}_{\eta_1,\eta_2} = \left\{ \mathbf{x} \in \mathbb{R}^2 : \eta_1 \leqslant \left| \operatorname{atan}\left(\frac{x_2}{x_1}\right) \right| \leqslant \eta_2 \right\}. \tag{8}$$

Here by atan we denote the extension of the arc tangent so that its range is $[0, 2\pi)$. Let $H_{\eta_1,\eta_2}(\mathbf{x}) = \chi_{\mathcal{W}_{\eta_1,\eta_2}}(\mathbf{x})$ denote the indicator function of such a wedge and assume without loss of generality that $0 < \eta_2 - \eta_1 < \pi$. The function H_{η_2,η_2} induces a distribution whose Fourier transform can be obtained by first computing the Fourier transform of $H_{0,\pi/2}$ and then squeezing and rotating the angular wedge $\mathcal{W}_{0,\pi/2}$ as required. The function $H_{0,\pi/2}$ is the indicator function of the first quadrant, and we have

$$H_{0,\pi/2}(\mathbf{x}) = \chi_{x_1>0}(x_1)\chi_{x_2>0}(x_2).$$

Thus, $H_{0,\pi/2}$ is a direct product of two Heaviside distributions. Therefore, its Fourier transform is also a direct product and is given as

$$\hat{H}_{0,\pi/2}(\xi) = \frac{1}{4}\delta(\xi_1)\delta(\xi_2) - \frac{\imath}{4\pi}\left(\delta(\xi_2)\mathrm{PV}\frac{1}{\xi_1} + \delta(\xi_1)\mathrm{PV}\frac{1}{\xi_2}\right) - \frac{1}{4\pi^2}\mathrm{PV}\frac{1}{\xi_1}\mathrm{PV}\frac{1}{\xi_2}, \tag{9}$$

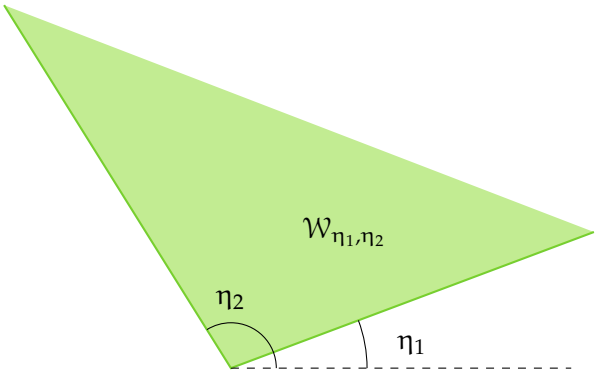

Figure 1: Angular wedge defined through its two angles, η_1 and η_2

where PV marks the Cauchy's principal value. In the rest of the text we will (mostly) omit writing PV for the sake of reducing the notational load, though it will always be lurking somewhere in the background. Denoting now

$$A = R_{\frac{\eta_2+\eta_1}{2}} \operatorname{diag}\left(1, \tan\left(\frac{\eta_2-\eta_1}{2}\right)\right) R_{\pi/4}, \tag{10}$$

we have $\mathcal{W}_{\eta_1,\eta_2} = A\,\mathcal{W}_{0,\pi/2}$. It follows

$$\hat{H}_{\eta_1,\eta_2}(\xi) = \tan\left(\frac{\eta_2-\eta_1}{2}\right) \hat{H}_{0,\pi/2}(A^\top \xi). \tag{11}$$

The case $\pi < \eta_1 - \eta_2 < 2\pi$ is analogous, since it follows from a simple observation of the identity $H_{\pi/2,2\pi} = 1 - H_{0,\pi/2}$.

We will first look at band-limited CPMs , where the computations are considerably simpler, yet they still give an indication of what needs to be done in the general case.

4.2 Band Limited Molecules

Let $\Gamma = \{m_\lambda : \lambda \in \Lambda_\Gamma\}$ be a CPM family and assume that for all λ the frequency support of $\varphi^{(\lambda)}$ satisfies

$$\operatorname{supp} \hat{\varphi}^{(\lambda)} \subseteq [A_1, A_2] \times [-B, B], \tag{12}$$

where $A_1, A_2, B > 0$ and $A_2 > A_1$. All known constructions of band-limited parabolic analysing systems satisfy support conditions of this type, consider for example second generation curvelets [5] and band-limited shearlets [16]. We can now show the following.

Lemma 4.2. *Let $\mathbf{p} = \mathbf{0} \in \mathbb{R}^2$, and $\Gamma = \{m_\lambda : \lambda \in \Lambda_\Gamma\}$ be a family of band-limited CPMs that satisfy (12) for all $\lambda \in \Lambda_\Gamma$. For $\lambda = (a_\lambda, \theta_\lambda, \mathbf{p})$ we then have*

$$\langle H_{\eta_1,\eta_2}, m_\lambda \rangle \lesssim a_\lambda^{5/4} \frac{\sin(\eta_2-\eta_1)}{\cos(\eta_1+\theta_\lambda)\cos(\eta_2+\theta_\lambda)},$$

when $\cos(\theta_\lambda + \eta_i) \neq 0$ for all $i = 1, 2$. On the other hand, if $\cos(\eta_j + \theta_\lambda) = 0$ we have

$$\langle H_{\eta_1,\eta_2}, m_\lambda \rangle \lesssim a_\lambda^{3/4} \frac{\sin(\eta_2-\eta_1)}{\cos(\eta_k+\theta_\lambda)},$$

where $k \in \{1, 2\} - j$.

Proof. Let us first examine the case when $\cos(\theta_\lambda + \eta_i) \neq 0$ for $i = 1, 2$. We can notice that the Dirac delta function contributions from (9), that is (11), vanish when the dilation

parameter a is small enough since the supports of the Dirac delta contributions (the origin) and $\widehat{\varphi}^{(\lambda)}$ do not intersect. Therefore, we have

$$\begin{aligned}\langle H_{\eta_1,\eta_2}, m_\lambda\rangle = \langle \widehat{H}_{\eta_1,\eta_2}, \widehat{m}_\lambda\rangle = \langle \widehat{H}_{0,\pi/2}, \widehat{m}_\lambda(A^\top\cdot)\rangle = c\cdot\int_{\mathbb{R}^2}\frac{\overline{\widehat{m}_\lambda}(A^\top\xi)}{\xi_1\xi_2}d\xi \\ = C\cdot\int_{\mathbb{R}^2}\frac{\overline{\widehat{\varphi}^{(\lambda)}}(\xi)d\xi}{(\xi_1+\sqrt{a_\lambda}\xi_2\tan(\eta_1+\theta_\lambda))(\xi_1+\sqrt{a_\lambda}\xi_2\tan(\eta_2+\theta_\lambda))},\end{aligned}$$

where

$$C = a_\lambda^{5/4}\frac{\sin(\eta_2-\eta_1)}{2\sqrt{2}\cos(\eta_1+\theta_\lambda)\cos(\eta_2+\theta_\lambda)}.$$

For $\xi\in\operatorname{supp}\widehat{\varphi}^{(\lambda)}\subseteq[A_1,A_2]\times[-B,B]$ we have that if the dilation parameter a is small enough, then $\xi_1+\sqrt{a_\lambda}\xi_2\tan(\eta_1+\theta_\lambda)$ and $\xi_1+\sqrt{a_\lambda}\xi_2\tan(\eta_2+\theta_\lambda)$ are uniformly away from 0, and moreover, are uniformly bounded from above and from below, which gives

$$\int_{\mathbb{R}^2}\frac{\overline{\widehat{\varphi}^{(\lambda)}}(\xi)d\xi}{(\xi_1+\sqrt{a_\lambda}\xi_2\tan(\eta_1+\theta_\lambda))(\xi_1+\sqrt{a_\lambda}\xi_2\tan(\eta_2+\theta_\lambda))}\lesssim\int_{\mathbb{R}^2}\overline{\widehat{\varphi}^{(\lambda)}}(\xi)d\xi\overset{(1)}{\lesssim}1.$$

Therefore,

$$\langle H_{\eta_1,\eta_2}, m_\lambda\rangle\lesssim a_\lambda^{5/4}\frac{\sin(\eta_2-\eta_1)}{\cos(\eta_1+\theta_\lambda)\cos(\eta_2+\theta_\lambda)}.$$

Let us now consider the other case. Without loss of generality, we assume $\cos(\eta_1+\theta_\lambda)=0$. The contribution of terms that involve $\delta(\xi_2)$ vanish using previous argumentation. Therefore, we are essentially left with an integral along one of the lines that define the angular wedge $\mathcal{W}_{\eta_1,\eta_2}$. Addresing that expression first we have

$$\begin{aligned}\left\langle\frac{1}{\xi_2}\delta(\xi_1),\widehat{m}_\lambda(A^\top\cdot)\right\rangle = c\cdot\int_{\mathbb{R}^2}\frac{\overline{\widehat{m}_\lambda}(A^\top\xi)}{\xi_2}\delta(\xi_1)d\xi = \tilde{C}\cdot\int_{\mathbb{R}^2}\frac{\delta(u_2)\overline{\widehat{\varphi}^{(\lambda)}}(u)}{u_1+\sqrt{a_\lambda}\tan(\eta_2+\theta_\lambda)u_2}du \\ \lesssim a_\lambda^{3/4}\frac{\sin(\eta_2-\eta_1)}{\cos(\eta_2+\theta_\lambda)},\end{aligned}$$

where $\tilde{C}=a_\lambda^{3/4}\frac{\sin(\eta_2-\eta_1)}{\cos(\eta_2+\theta_\lambda)}$. Analogous analysis gives

$$\left\langle\frac{1}{\xi_1\xi_2},\widehat{m}_\lambda(A^\top\cdot)\right\rangle\lesssim a_\lambda^{3/4}\frac{\sin(\eta_2-\eta_1)}{\cos(\eta_2+\theta_\lambda)}\int_{\mathbb{R}^2}\frac{\overline{\widehat{\varphi}^{(\lambda)}(\xi)}}{\xi_2}d\xi,$$

where the integral is finite due to the assumptions on $\widehat{\varphi}^{(\lambda)}$. Therefore, putting it all together we have

$$\langle H_{\eta_1,\eta_2}, m_\lambda\rangle\lesssim a_\lambda^{3/4}\frac{\sin(\eta_2-\eta_1)}{\cos(\eta_2+\theta_\lambda)},$$

as desired. □

For full disclosure, the rate $a^{3/4}$ can up to a multiplicative constant be reached by the same arguments as in (5), that is, by considering the L^∞ nature of the Heaviside function. But, in Lemma 4.2 we obtain further information about the geometric interplay between the orientation of the molecule and the angles at the corner point.

4.3 General Parabolic Molecules

We will now show that the results of the previous section can be extended to more general scenarios, namely, for CPMs that are not necessarily band-limited. Even though the general principles remain the same, the computations will get significantly more delicate and we will need to impose some rather mild conditions on the CPM family we will be

working with. In this section we will constantly work under the assumption that the underlying CPM family is of sufficiently high order (R, M, N_1, N_2), since our focus is not on deriving precise and quantifiable estimates. We hope that this will be clear in every proof and statement.

Let us first recall that the Fourier transform of H_{η_1,η_2} is given by

$$\hat{H}_{\eta_1,\eta_2}(\xi) = \tan\left(\frac{\eta_2-\eta_1}{2}\right)\hat{H}_{0,\pi/2}(A^\top\xi),$$

where

$$\hat{H}_{0,\pi/2}(\xi) = \frac{1}{4}\delta(\xi_1)\delta(\xi_2) - \frac{\iota}{4\pi}\left(\delta(\xi_2)\mathrm{PV}\frac{1}{\xi_1} + \delta(\xi_1)\mathrm{PV}\frac{1}{\xi_2}\right) - \frac{1}{4\pi^2}\mathrm{PV}\frac{1}{\xi_1}\mathrm{PV}\frac{1}{\xi_2},$$

with A as defined in (10). To simplify the notation for the computations, let us split $\langle H_{\eta_1,\eta_2}, m_\lambda\rangle$ into three terms as follows,

$$\begin{aligned}\langle H_{\eta_1,\eta_2}, m_\lambda\rangle &= \langle \hat{H}_{\eta_1,\eta_2}, \hat{m}_\lambda\rangle = \langle \hat{H}_{0,\pi/2}, \hat{m}_\lambda(A^\top\cdot)\rangle \\ &= \frac{1}{4}\langle H_1, \hat{m}_\lambda(A^\top\cdot)\rangle - \frac{\iota}{4\pi}\langle H_2, \hat{m}_\lambda(A^\top\cdot)\rangle - \frac{1}{4\pi^2}\langle H_3, \hat{m}_\lambda(A^\top\cdot)\rangle,\end{aligned}$$

where (omitting PV) we define

$$\begin{aligned} H_1(\xi) &= \delta(\xi_1)\delta(\xi_2), \\ H_2(\xi) &= \frac{\delta(\xi_1)}{\xi_2} + \frac{\delta(\xi_2)}{\xi_1}, \\ H_3(\xi) &= \frac{1}{\xi_1\xi_2}. \end{aligned} \tag{13}$$

Let us first address the case when the molecule m_λ is not orthogonal to either sides of the wedge. In contrast with the discussion in Section 4.2, the action of the distribution $\hat{H}_{\eta_1,\eta_2}$ on a function $\hat{\varphi}^{(\lambda)}$, whose support is not necessarily compact, will generally include the contributions of all three terms, H_1, H_2 and H_3. In order to see this, we can start by observing the contribution of the first term.

Lemma 4.3. *Consider a CPM family $\Gamma = \{m_\lambda : \lambda \in \Lambda_\Gamma\}$ of order (R, M, N_1, N_2) and the distribution H_1 defined in (13). Provided the dilation parameter a_λ is small enough we have*

$$\langle H_1, \hat{m}_\lambda(A^\top\cdot)\rangle \lesssim a_\lambda^{3/4+M}, \tag{14}$$

where the matrix A is defined in (10).

Proof. A simple computation gives

$$\langle \delta(\xi_1)\delta(\xi_2), \hat{m}_\lambda(A^\top\cdot)\rangle \sim a_\lambda^{3/4}\hat{\varphi}^{(\lambda)}(\mathbf{0}) \leqslant a_\lambda^{M+3/4}, \tag{15}$$

where we used (1). □

Notice that for band-limited molecules that obey support assumptions (12) the left hand side of (14) would be equal to 0 since the origin is not in the support of $\hat{\varphi}^{(\lambda)}$.

Let us now look at the second term.

Lemma 4.4. *Consider a CPM family $\Gamma = \{m_\lambda : \lambda \in \Lambda_\Gamma\}$ and the distribution H_2 defined in (13). Provided the dilation parameter a_λ is small enough we have*

$$\langle H_2, \hat{m}_\lambda(A^\top\cdot)\rangle \lesssim a_\lambda^{5/4+C_{M,N_1}}, \tag{16}$$

where $C_{M,N_1} > 0$ is a positive constant that depends on the order of family Γ, and becomes arbitrarily large provided M and N_1 are big enough, and matrix A is defined in (10).

Proof. Consider first the action of $\frac{1}{\xi_2}\delta(\xi_1)$ and omit the indices. The other term can be treated analogously. We have

$$\left\langle \frac{1}{\xi_2}\delta(\xi_1), \hat{\mathfrak{m}}(A^\top \cdot) \right\rangle = a^{3/4} \int_{\mathbb{R}^2} \frac{1}{\xi_2}\delta(\xi_1)\overline{\hat{\varphi}}(T\xi)\mathrm{d}\xi,$$

where $T = D_a R_\theta A^\top$, with A. Denote now

$$f(y) := \overline{\hat{\varphi}}\left(y(a\cos(\theta+\eta_1), \sqrt{a}\sin(\theta+\eta_1)\right) = \hat{\varphi}(\tilde{\mathbf{y}}).$$

If we apply the Dirac delta and use the change of variables

$$\xi_2 \mapsto \frac{y}{\sqrt{2}\cos\left(\frac{\eta_2-\eta_1}{2}\right)},$$

it follows

$$\left\langle \frac{1}{\xi_2}\delta(\xi_1), \hat{\mathfrak{m}}(A^\top \cdot) \right\rangle \sim a^{3/4} \int_{\mathbb{R}} \frac{f(y)}{y}\mathrm{d}y.$$

Following the standard proof of well-definedness of Cauchy's principal value, we can split up the integral as

$$\int_{|y|>\epsilon} f(y)\frac{1}{y}\mathrm{d}y = \int_{|y|>\epsilon}^{C} f(y)\frac{1}{y}\mathrm{d}y + \int_{|y|>C}^{\infty} f(y)\frac{1}{y}\mathrm{d}y, \tag{17}$$

where $C > 0$ is a constant that will be specified later. In order to bound the first term we observe

$$\int_{|y|>\epsilon}^{C} \frac{f(y)}{y}\mathrm{d}y = \int_{y>\epsilon}^{C} \frac{f(y)-f(-y)}{y}\mathrm{d}y \leqslant 2C \cdot \sup_{y\in[0,C]} |f'(y)|, \tag{18}$$

which follows from the continuity and the mean value theorem. To bound $f'(y)$ we have by the chain rule

$$|f'(y)| \leqslant \|\partial\hat{\varphi}(\tilde{\mathbf{y}})\|\|\nabla\tilde{\mathbf{y}}\| \leqslant a^{1/2}\|\partial\hat{\varphi}(\tilde{\mathbf{y}})\|.$$

Take $C > 0$ to be such that $1 + |y| \leqslant a^{-\beta}$ holds for all $y \in [0, C]$ and some $\beta > 0$ which will be discussed later. Notice that this implies $C \sim a^{-\beta}$. We now have

$$|f'(y)| \lesssim a^{1/2}\min(1, a(1+|y|))^M \leqslant a^{1/2+M(1-\beta)}, \tag{19}$$

using the moment condition from (1). Plugging (19) into (18) it follows

$$\int_{|y|>\epsilon}^{C} \frac{f(y)}{y}\mathrm{d}y \lesssim a^{M(1-\beta)-\beta+1/2}. \tag{20}$$

On the other hand, we can write

$$\int_{|y|>C} \frac{f(y)}{y}\mathrm{d}y = \int_{|y|>C} \frac{yf(y)}{y^2}\mathrm{d}y \lesssim C^{-1} \sup_{y\in[C,\infty)} |yf(y)|. \tag{21}$$

Furthermore, since we now have $1 + |y| \geqslant a^{-\beta}$ it follows $1+|y|^2 \geqslant \frac{a^{-2\beta}}{2}$. Thus, using the decay conditions (1) we have $|\hat{\varphi}(\tilde{\mathbf{y}})| \lesssim \langle\|\tilde{\mathbf{y}}\|\rangle^{-N_1}\langle\tilde{\mathbf{y}}_2\rangle^{-1}$, which yields

$$|yf(y)| \leqslant a^{-1}\langle\tilde{\mathbf{y}}_2\rangle|\hat{\varphi}(\tilde{\mathbf{y}})| \leqslant a^{-1}\langle\|\tilde{\mathbf{y}}\|\rangle^{-N_2} \lesssim a^{N_1(2\beta-1)-1}. \tag{22}$$

Therefore, plugging (22) into (21) we have

$$\int_{|y|>C} \frac{f(y)}{y}\mathrm{d}y \lesssim a^{N_1(2\beta-1)+\beta-1}. \tag{23}$$

Looking at equations (20) and (23) we see that we need $1/2 < \beta < 1$. Therefore, provided M and N_1 are both large enough, the terms in (20) and (23) will have arbitrarily fast decay. To be more precise, in order to ensure that the decay rate is faster than $5/4$ we need

$$M \geqslant \frac{3/4+\beta}{1-\beta} \text{ and } N_1 \geqslant \frac{9/4-\beta}{2\beta-1}.$$

An entirely analogous argument yields the same decay order for the other term, $\langle \frac{1}{\xi_1}\delta(\xi_2), \widehat{m}_\lambda(A^\top \cdot)\rangle$. Hence, the conclusion follows. □

Estimates (14) and (16) say that the terms $\langle H_1, m_\lambda\rangle$ and $\langle H_2, m_\lambda\rangle$ exhibit fast decay which depends on the smoothness of the molecule. Let us now address the last remaining term. First, we need to define vanishing moments.

Definition 4.2. We say that a bivariate function $f \in L^2(\mathbb{R}^2)$ has K *vanishing moments in the* x_j *direction*, where $K \in \mathbb{N}$ and $j \in \{1,2\}$, if

$$\int_{\mathbb{R}^2} \frac{|\widehat{f}(\xi)|^2}{|\xi_j|^{2K}} d\xi < \infty. \tag{24}$$

Lemma 4.5. *Consider a CPM family* $\Gamma = \{m_\lambda : \lambda \in \Lambda_\Gamma\}$ *such that the functions* $\varphi^{(\lambda)}$ *have one vanishing moment in the* x_1 *direction, the distribution* H_3 *defined in (13), and consider the matrix* A *as defined in (10). Provided the dilation parameter* a *is small enough, we have*

$$\langle H_3, \widehat{m}_\lambda(A^\top \cdot)\rangle \lesssim a_\lambda^{5/4} \frac{\sin(\eta_2-\eta_1)}{\cos(\eta_1+\theta_\lambda)\cos(\eta_2+\theta_\lambda)}.$$

Proof. Let us omit the indices and notice that same as in Section 4.2 we have

$$\left\langle \frac{1}{\xi_1\xi_2}, \widehat{m}(A^\top)\right\rangle = C\int_{\mathbb{R}^2} \frac{\overline{\widehat{\varphi}}(\xi)d\xi}{(\xi_1+\sqrt{a}\xi_2\tan(\eta_1+\theta))(\xi_1+\sqrt{a}\xi_2\tan(\eta_2+\theta))}, \tag{25}$$

where

$$C = a^{5/4}\frac{\sin(\eta_2-\eta_1)}{2\sqrt{2}\cos(\eta_1+\theta)\cos(\eta_2+\theta)}.$$

The integral in (25) can be split in three parts. The first part is the integral over $\left|\frac{\xi_2}{\xi_1}\right| \leqslant a^{-\alpha}$, where we write $\alpha = \frac{1}{2}-\varepsilon > 0$. Denote $t_i = \tan(\eta_i+\theta)$. We have

$$1-|t_i|a^\varepsilon \leqslant \left|1+t_i\sqrt{a}\frac{\xi_2}{\xi_1}\right| \leqslant 1+|t_i|a^\varepsilon. \tag{26}$$

Hence, provided the dilation parameter a is small enough it follows

$$\frac{1}{\xi_1+\sqrt{a}t_1\xi_2}, \frac{1}{\xi_1+\sqrt{a}t_2\xi_2} \sim \frac{1}{\xi_1}.$$

Therefore,

$$\int_{\left|\frac{\xi_2}{\xi_1}\right|\leqslant a^{-\alpha}} \frac{\overline{\widehat{\varphi}}(\xi)d\xi}{(\xi_1+\sqrt{a}t_1\xi_2)(\xi_1+\sqrt{a}t_2\xi_2)} \sim \int_{\left|\frac{\xi_2}{\xi_1}\right|\leqslant a^{-\alpha}} \frac{\overline{\widehat{\varphi}}(\xi)d\xi}{\xi_1^2}, \tag{27}$$

which is finite since we assumed φ satisfies the vanishing moments condition.

Consider now the contribution coming from the integral over $\left|\frac{\xi_2}{\xi_1}\right| \geqslant a^{-\alpha}$. Let us first observe the change of variables under the linear transformation

$$\xi \mapsto \mathbf{v} = \begin{pmatrix} 1 & \sqrt{a}t_1 \\ 1 & \sqrt{a}t_2 \end{pmatrix}\xi. \tag{28}$$

Applying (28) gives

$$\int_{\left|\frac{\xi_2}{\xi_1}\right|\geqslant a^{-\alpha}} \frac{\overline{\widehat{\varphi}}(\xi)d\xi}{(\xi_1+\sqrt{a}t_1\xi_2)(\xi_1+\sqrt{a}t_2\xi_2)} = \frac{a^{-1/2}}{|t_2-t_1|}\int_{\left|\frac{\xi_2}{\xi_1}\right|\geqslant a^{-\alpha}} \frac{\widehat{\varphi}^a_{t_2t_1}(\mathbf{v})}{v_1v_2}dv_1dv_2, \tag{29}$$

where $\widehat{\varphi}^a_{t_2t_1}$ is defined as

$$\widehat{\varphi}^a_{t_2t_1}(\mathbf{v}) = \overline{\widehat{\varphi}}\left(\frac{1}{t_2-t_1}(t_2v_1-t_1v_2, a^{-1/2}(v_2-v_1)\right).$$

We will now split the area of integration in the integral (29) in two pieces. The first piece is the box $I_{a,\gamma}=[-a^\gamma,a^\gamma]^2$, for $\gamma>0$ that will be specified later. Applying the standard methods of Cauchy's principal value we have

$$\frac{a^{-1/2}}{|t_2-t_1|}\int_{I_{a,\gamma}}\frac{\widehat{\varphi}^a_{t_2t_1}(\mathbf{v})}{v_1v_2}d\mathbf{v} \lesssim \frac{a^{-1/2}}{|t_2-t_1|}\int_{I_{a,\gamma}}\sup_{\tilde{\mathbf{v}}\in I_{a,\gamma}}|\partial^{(1,1)}\left(\widehat{\varphi}^a_{t_2t_1}(\tilde{\mathbf{v}})\right)|d\mathbf{v}. \tag{30}$$

The chain rule gives

$$\left|\partial^{(1,1)}\left(\widehat{\varphi}^a_{t_2t_1}(\mathbf{v})\right)\right| \lesssim a^{-1}\max_{|\boldsymbol{\alpha}|=2}\left|\partial^{\boldsymbol{\alpha}}\widehat{\varphi}\left(\frac{1}{t_2-t_1}(t_2v_1-t_1v_2, a^{-1/2}(v_2-v_1))\right)\right|,$$

where $\boldsymbol{\alpha}\in\mathbb{N}_0^2$ is a multi-index. This can be bounded using (1) as

$$\left|\partial^{\boldsymbol{\alpha}}\widehat{\varphi}\Big(\frac{1}{t_2-t_1}(t_2v_1-t_1v_2, a^{-1/2}(v_2-v_1)\Big)\right| \lesssim \left(a+\frac{|t_2v_1-t_1v_2|+|v_2-v_1|}{|t_2-t_1|}\right)^M.$$

Therefore,

$$\left|\partial^{\boldsymbol{\alpha}}\widehat{\varphi}\left(\frac{1}{t_2-t_1}(t_2v_1-t_1v_2, a^{-1/2}(v_2-v_1))\right)\right| \lesssim a^{M\gamma}, \quad \text{for all } \mathbf{v}\in I_{a,\gamma}.$$

Plugging it back into (30) we get

$$\frac{a^{-1/2}}{|t_2-t_1|}\int_{I_{a,\gamma}}\frac{\widehat{\varphi}^a_{t_2t_1}(\mathbf{v})}{v_1v_2}d\mathbf{v} \lesssim a^{M\gamma+2\gamma-3/2}. \tag{31}$$

Consider now the image of the cone $\left|\frac{\xi_2}{\xi_1}\right|\geqslant a^{-\alpha}$ under the linear transformation defined by (28). The result is the cone $\mathcal{C}^a_{t_1,t_2}$ that is determined by the lines through the points $(\pm1\pm a^\epsilon t_1, \pm1\pm a^\epsilon t_2)$. Therefore, we can decompose it four equivalent pieces.

Let us assume now, without loss of generality, that $t_1>t_2$. It follows

$$\frac{a^{-1/2}}{|t_2-t_1|}\int_{\mathcal{C}^a_{t_1t_2}-I_{a,\gamma}}\frac{\widehat{\varphi}^a_{t_2t_1}(\mathbf{v})}{v_1v_2}d\mathbf{v} \lesssim a^{-1/2-2\gamma}\int_{v_2=a^\gamma}^{\infty}\int_{v_1=-v_2}^{(1-a^\epsilon)v_2}|\widehat{\varphi}^a_{t_1,t_2}(\mathbf{v})|d\mathbf{v}.$$

We can now use the decay estimate $|\partial^{\boldsymbol{\alpha}}\widehat{\varphi}(\mathbf{v})|\lesssim|v_2|^{-N_2}$, which yields

$$\begin{aligned}\frac{a^{-1/2}}{|t_2-t_1|}\int_{\mathcal{C}^a_{t_1t_2}-I_{a,\gamma}}\frac{\widehat{\varphi}^a_{t_2t_1}(\mathbf{v})}{v_1v_2}d\mathbf{v} &\lesssim a^{-1/2+N_2/2-2\gamma}\int_{\mathcal{C}^a_{t_1t_2}-I_{a,\gamma}}|v_2-v_1|^{-N_2}d\mathbf{v}\\ &\lesssim a^{N_2\left(\frac12-(\gamma+\epsilon)\right)+\epsilon-1/2}.\end{aligned} \tag{32}$$

Let us recollect the requirements on γ and ϵ. First of all, we need $\gamma,\epsilon>0$, whereas (26) and (32) further impose $\epsilon<1/2$ and $\gamma+\epsilon<1/2$. Choosing γ and ϵ that satisfy these conditions, we have fast decay provided M and N_2 are big enough and the statement follows from (27), (31) and (32). □

We can combine the three preceding lemmas in the following theorem.

Theorem 4.6. *Assume* $\Gamma = \{m_\lambda : \lambda \in \Lambda_\Gamma\}$ *is a family of CPMs . Let* $\lambda = (a_\lambda, \theta_\lambda, \mathbf{p})$ *be such that* θ_λ *is orthogonal to neither* η_2 *nor* η_1*. Then we have*

$$\langle H_{\eta_1,\eta_2}, m_\lambda \rangle \lesssim a_\lambda^{5/4} \frac{\sin(\eta_2 - \eta_1)}{\cos(\eta_1 + \theta_\lambda)\cos(\eta_2 + \theta_\lambda)} + a^{C_{M,N_1,N_2}},$$

where $C_{M,N_1,N_2} > 0$ *is a positive constant that depends on* M, N_1 *and* N_2*, is greater than* $5/4$ *and becomes arbitrarily large for large* M, N_1 *and* N_2*.*

Proof. We have

$$\langle H_{\eta_1,\eta_2}, m_\lambda \rangle = \frac{1}{4}\langle H_1, \widehat{m}_\lambda(A^\top \cdot)\rangle - \frac{\iota}{4\pi}\langle H_2, \widehat{m}_\lambda(A^\top \cdot)\rangle - \frac{1}{4\pi^2}\langle H_3, \widehat{m}_\lambda(A^\top \cdot)\rangle,$$

where H_1, H_2 and H_3 are as defined in (13). The statement then follows by using the triangle inequality and applying Lemmas 4.3, 4.4 and 4.5. □

An analogous analysis can be applied to the case when the parabolic molecule is aligned with one of the wedge lines. We will not provide the details here since the calculations are very similar to those we have already performed and since essentially the same decay rate can be again obtained by merely using the L^∞ nature of H_{η_1,η_2}.

Theorem 4.7. *Assume* $\Gamma = \{m_\lambda : \lambda \in \Lambda_\Gamma\}$ *is a family of CPMs . Let* $\lambda = (a_\lambda, \theta_\lambda, \mathbf{p})$ *be such that* $\cos(\eta_j + \theta_\lambda) = 0$*, and consider* $k \in \{1, 2\} - j$*. Then we have*

$$\langle H_{\eta_1,\eta_2}, m_\lambda \rangle \lesssim a_\lambda^{3/4} \frac{\sin(\eta_2 - \eta_1)}{\cos(\eta_k + \theta)} + a^{C_{M,N_1,N_2}},$$

where $C_{M,N_1,N_2} > 0$ *depends on* M, N_1 *and* N_2*, and is greater than* $3/4$ *and becomes arbitrarily large for large* M, N_1 *and* N_2*.*

4.4 Polygons

The tools we developed thus far allow us to identify the corner points of polygons. To begin, let us show that translating any given set does not affect the decay rates. Taking a set $\Omega \subseteq \mathbb{R}^2$ and a point $\mathbf{p} \in \mathbb{R}^2$, it follows

$$\chi_{\Omega+\mathbf{p}}(\mathbf{x}) = \chi_\Omega(\mathbf{x} - \mathbf{p}) = T_\mathbf{p}\chi_\Omega(\mathbf{x}),$$

where $T_\mathbf{p}$ denotes the translation operator. Since the Fourier transform maps translations into modulations, we have

$$\begin{aligned}
\langle \chi_{\Omega+\mathbf{p}}, m_\lambda \rangle &= \langle \hat{\chi}_{\Omega+\mathbf{p}}, \widehat{m}_\lambda \rangle \\
&= \int_{\mathbb{R}^2} e^{-2\pi\iota\xi\cdot\mathbf{p}} \hat{\chi}_\Omega(\xi) e^{2\pi\iota\xi\cdot\mathbf{p}} \overline{\hat{\varphi}^{(\lambda)}}(D_{a_\lambda} R_{\theta_\lambda}\xi) d\xi \\
&= \int_{\mathbb{R}^2} \hat{\chi}_\Omega(\xi) \overline{\hat{\varphi}^{(\lambda)}}(D_{a_\lambda} R_{\theta_\lambda}\xi) d\xi
\end{aligned}$$

where $\lambda = (a_\lambda, \theta_\lambda, \mathbf{p})$. Therefore, as expected, translating the set does not affect the decay rates of the frame coefficients, and it is sufficient to restrict our attention to the study of the decay rates for $\mathbf{p} = \mathbf{0}$.

Consider now a polygon $\mathcal{P}$ and a corner point $\mathbf{p}$ on its boundary and let η_1 and η_2 be the angles determined by the two lines of the polygon that meet at $\mathbf{p}$. Using the localisation Lemma 4.1 it follows that the decay rates of coefficients $\langle \chi_\mathcal{P}, m_\lambda \rangle$ are the same as those of $\langle H_{\eta_1,\eta_2}, m_\lambda \rangle$. Therefore, we can apply the results from Section 4.3. We can summarise these findings in the following theorem.

Theorem 4.8. *Let $\mathcal{P} \subseteq \mathbb{R}^2$ be a polygon and $\Gamma = \{m_\lambda : \lambda \in \Lambda_\Gamma\}$ a family of continuous parabolic molecules. Consider $\mathbf{p} \in \partial\mathcal{P}$. Provided $\mathbf{p}$ is a corner point of $\mathcal{P}$ and $\lambda = (a_\lambda, \theta_\lambda, \mathbf{p})$ then if θ_λ is not orthogonal to $\partial\mathcal{P}$ at $\mathbf{p}$, we have*

$$\langle \chi_{\mathcal{P}}, m_\lambda \rangle \lesssim a_\lambda^{5/4} \frac{\sin(\eta_2 - \eta_1)}{\cos(\eta_1 + \theta_\lambda)\cos(\eta_2 + \theta_\lambda)},$$

and otherwise if $\cos(\eta_j + \theta_\lambda) = 0$, then for $k \in \{1, 2\} - j$ we have

$$\langle \chi_{\mathcal{P}}, m_\lambda \rangle \lesssim a_\lambda^{3/4} \frac{\sin(\eta_2 - \eta_1)}{\cos(\eta_k + \theta_\lambda)}.$$

Proof. Since $H_{\eta_1,\eta_2} = \chi_{\mathcal{P}}$ in the neighbourhood of $\mathbf{p}$, by the localisation Lemma 4.1 we have that $\langle \chi_{\mathcal{P}}, m_\lambda \rangle$ is of the same decay order as $\langle H_{\eta_1,\eta_2}, m_\lambda \rangle$. The result now follows directly from Theorems 4.6 and 4.7. □

4.5 General Sets

In order to detect edges and corner points of general sets we will now use a fairly straightforward approximation argument. The boundary of a given corner point of $\partial\Omega$ will be locally approximated using straight lines whose orientations are determined by the tangents at the corner point. It will then follow that such an approximating procedure preserves the decay rates. Therefore, decay rates that we have computed for angular wedges will give decay rates on domains with more general boundaries.

Assume again that $\Omega \subseteq \mathbb{R}^2$ is a bounded and open set with continuous and piecewise-smooth boundary that has and bounded curvature, and is parametrised by $\alpha_\Omega : [0, 1] \to \mathbb{R}^2$. Consider a corner point $\mathbf{p} \in \partial\Omega$ where $\mathbf{p} = \alpha_\Omega(t_0)$ with $\alpha'_\Omega(t_0^+) \neq \pm\alpha'_\Omega(t_0^-)$. Let $\epsilon > 0$ be small enough so that $\mathcal{B}_\epsilon(\mathbf{p})$ intersects $\partial\Omega$ at exactly 2 points (the same then holds for all smaller ϵ). Let $\mathcal{R}$ denote the set that approximates Ω. For the points outside of $\mathcal{B}_\epsilon(\mathbf{p})$, the set $\mathcal{R}$ is equal to Ω, that is

$$\mathcal{R} - \mathcal{B}_\epsilon(\mathbf{p}) = \Omega - \mathcal{B}_\epsilon(\mathbf{p}).$$

On the other hand, part of the boundary $\partial\mathcal{R}$ within $\mathcal{B}_\epsilon(\mathbf{p})$ is a linear approximation of α_Ω obtained by locally replacing the boundary of $\partial\Omega$ with tangent lines emanating from $\mathbf{p}$ (look at Figure 4.5). That is, from the left we use $\alpha'_\Omega(t_0^-)$ and from the right $\alpha'_\Omega(t_0^+)$, to be the slopes of the respective linear interpolants through $\mathbf{p}$ (we assume α_Ω takes a positive orientation). We will denote the parametrisation of the $\partial\mathcal{R}$ as $\alpha_\mathcal{R}$. What is important is that in $\mathcal{B}_\epsilon(\mathbf{p})$ [16] we have

$$\|\alpha_\Omega(t) - \alpha_\mathcal{R}(t)\| \leqslant C(t - t_0)^2.$$

The first step in our approximation procedure is to show that the linear approximation $\chi_\mathcal{R}$ exhibits the same decay rates at $\mathbf{p}$ as its corresponding translated angular wedge $\mathcal{W}_{\eta_1,\eta_2} + \mathbf{p}$, where η_1 and η_2 denote the angles defined by the tangents $\alpha'_\Omega(t_0^+)$ and $\alpha'_\Omega(t_0^-)$. By the discussion at the beginning of Section 4.4, we can without loss of generality assume $\mathbf{p} = \mathbf{0}$. Furthermore, in the following we will assume that we are working with a CPM family $\Gamma = \{m_\lambda : \lambda \in \Lambda_\Gamma\}$ which is of sufficiently high order.

Lemma 4.9. *Let $\chi_\mathcal{R}$ be the local approximation of the set Ω that we just described, and let the angles η_1 and η_2 correspond to the tangents $\alpha'_\Omega(t_0^+)$ and $\alpha'_\Omega(t_0^-)$. Then the following holds*

$$\text{if for } \rho > 0 \quad \langle H_{\eta_1,\eta_2}, m_\lambda \rangle \lesssim a_\lambda^\rho, \text{ as } a_\lambda \to 0, \text{ then } \langle \chi_\mathcal{R}, m_\lambda \rangle \lesssim a_\lambda^\rho, \text{ as } a_\lambda \to 0,$$

where $\lambda = (a_\lambda, \theta_\lambda, \mathbf{p})$.

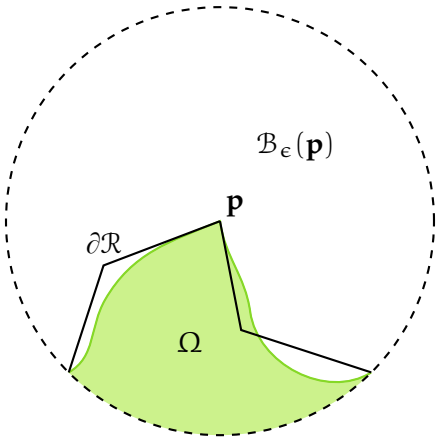

Figure 2: Local approximation of the boundary around a corner point

Proof. We have

$$\langle \chi_{\mathcal{R}}, m_\lambda \rangle = \langle H_{\eta_1,\eta_2}, m_\lambda \rangle + \langle \chi_{\mathcal{R}} - H_{\eta_1,\eta_2}, m_\lambda \rangle.$$

Therefore, since $H_{\eta_1,\eta_2} = \chi_{\mathcal{R}}$ holds on $\mathcal{B}_{\epsilon/2}(\mathbf{p})$, the localisation Lemma 4.1 gives

$$\langle \chi_{\mathcal{R}} - H_{\eta_1,\eta_2}, m_\lambda \rangle \lesssim a^N,$$

for every $N \in \mathbb{N}$ for which $\Delta^N \hat{\varphi}$ exists and has a finite L^1 norm. Since we by assumption have $\langle H_{\eta_1,\eta_2}, m_\lambda \rangle \leqslant \tilde{C} a^\rho$, the statement follows (provided $N \geqslant \rho$). □

Notice now

$$\langle \chi_\Omega, m_\lambda \rangle = \langle \chi_{\mathcal{R}}, m_\lambda \rangle + \langle \chi_\Omega - \chi_{\mathcal{R}}, m_\lambda \rangle. \tag{33}$$

Let us focus on the second term.

Lemma 4.10. *Let Ω and $\mathcal{R}$ be the previously described sets. Then for a CPM family $\Gamma = \{m_\lambda : \lambda \in \Lambda_\Gamma\}$, we have*

$$\langle \chi_\Omega - \chi_{\mathcal{R}}, m_\lambda \rangle \lesssim a_\lambda^{C_N},$$

where $C_N > \frac{5}{4}$ and $\lambda = (a_\lambda, \theta_\lambda, \mathbf{p})$.

Proof. Let us omit the λ indices. We have

$$\langle \chi_\Omega - \chi_{\mathcal{R}}, m \rangle = \underbrace{\int_{\mathcal{B}_{a^\gamma}(\mathbf{p})} m(\mathbf{x}) (\chi_\Omega - \chi_{\mathcal{R}})(\mathbf{x}) d\mathbf{x}}_{I_1} + \underbrace{\int_{\mathcal{B}^c_{a^\gamma}(\mathbf{p})} m(\mathbf{x}) (\chi_\Omega - \chi_{\mathcal{R}})(\mathbf{x}) d\mathbf{x}}_{I_2}.$$

where $\gamma > 0$, and will be specified later, and a is taken small enough so that $a^\gamma < \epsilon$ is ensured. We will approach the discussion in slightly broader generality by allowing $\|\alpha_\Omega(t) - \alpha_{\mathcal{R}}(t)\| \leqslant C|t - t_0|^k$ for some $k \in \mathbb{N}$. Furthermore, we will denote the desired decay rate with q. We would like to see how does the interaction between k and q play out.

Estimating I_1 we have

$$\begin{aligned} |I_1| &\lesssim a^{-3/4} \int_{\mathcal{B}_{a^\gamma}(\mathbf{p})} |\chi_\Omega - \chi_{\mathcal{R}}|(\mathbf{x}) d\mathbf{x} \lesssim a^{-3/4} \int_{t_0 - a^\gamma}^{t_0 + a^\gamma} \|\alpha_\Omega(t) - \alpha_{\mathcal{R}}(t)\| dt \\ &\lesssim a^{-3/4} \int_{t_0 - a^\gamma}^{t_0 + a^\gamma} |t_0 - t|^k dt \lesssim a^{-3/4 + \gamma(k+1)}. \end{aligned}$$

Hence, we need $-3/4+\gamma(k+1) > q$. Since $\Omega - \mathcal{B}_\epsilon(\mathbf{p}) = \mathcal{R} - \mathcal{B}_\epsilon(\mathbf{p})$, we can estimate I_2 by

$$\begin{aligned}|I_2| &\lesssim \int_{\mathcal{B}^c_{a^\gamma}(\mathbf{p})} |\varphi(M(\mathbf{x}-\mathbf{p}))||\chi_\Omega - \chi_\mathcal{R}|(\mathbf{x})d\mathbf{x} \lesssim a^{-3/4}\int_{\mathcal{B}_\epsilon(\mathbf{p})-\mathcal{B}_{a^\gamma}(\mathbf{p})} |\varphi(M(\mathbf{x}-\mathbf{p}))|d\mathbf{x} \\ &\lesssim a^{-3/4}\int_{\mathcal{B}_\epsilon(\mathbf{p})-\mathcal{B}_{a^\gamma}(\mathbf{p})} |\varphi(D_{1/a}(\mathbf{x}-\mathbf{p}))|d\mathbf{x},\end{aligned}$$

where $M = D_{1/a}R_\theta$. Using (7), we now have

$$\begin{aligned}|I_2| &\lesssim a^{-3/4}\int_{\mathcal{B}_\epsilon(\mathbf{p})-\mathcal{B}_{a^\gamma}(\mathbf{p})} \left(1 + a^{-2}x_1^2 + a^{-1}x_2^2\right)^{-N} d\mathbf{x} \lesssim \epsilon a^{2N-3/4}\int_{a^\gamma}^\infty x_1^{-2N}dx_1 \\ &\lesssim \epsilon a^{2N(1-\gamma)-3/4+\gamma}.\end{aligned}$$

Therefore, for the statement to hold we need $2N(1-\gamma) - 3/4 + \gamma > q$, which is the case provided $\gamma < 1$ and provided N is big enough.

Getting back to the statement of the lemma, for $q = 5/4$, we would need $\gamma > \frac{2}{k+1}$ and $\gamma < 1 - \frac{1}{2N-1}$. Furthermore, since we are using linear interpolation through $\mathcal{R}$ in order to locally approximate Ω, we have $k = 2$. It follows that $\gamma > \frac{2}{3}$. Therefore, such a γ will exist provided $N \geqslant 3$. □

We can now combine the previous lemmas into the following theorem.

Theorem 4.11. *Let $\Omega \subseteq \mathbb{R}^2$ be a bounded and open set with continuous and piecewise-smooth boundary that has bounded curvature. Assume $\Gamma = \{m_\lambda : \lambda \in \Lambda_\Gamma\}$ is a family of continuous parabolic molecules which satisfy the assumptions of Lemmas 4.9 and 4.10. If $\mathbf{p}$ is a corner point of Ω, them omitting the higher order terms we have*

$$\langle \chi_\Omega, m_\lambda\rangle \lesssim a_\lambda^{5/4},$$

when $\lambda = (a_\lambda, \theta_\lambda, \mathbf{p})$ and θ_λ is orthogonal to neither $\alpha'_\Omega(t_0^+)$ nor $\alpha'_\Omega(t_0^-)$, where $\alpha_\Omega(t_0) = \mathbf{p}$. Otherwise, if θ_λ is orthogonal to $\partial\Omega$ at $\mathbf{p}$ we have

$$\langle \chi_\Omega, m_\lambda\rangle \lesssim a_\lambda^{3/4}.$$

Proof. Let η_1 and η_2 be the angles associated with the tangents, $\alpha'(t_0^+)$ and $\alpha'(t_0^-)$, at $\mathbf{p} \in \partial\Omega$, and assume without loss of generality that $\mathbf{p} = \mathbf{0}$. Since $\mathbf{p}$ is a corner point we have $\eta_2 - \eta_2 \notin \pi\mathbb{Z}$ by assumption. Consider first the case when θ_λ is orthogonal to neither η_1 nor η_2. By Lemma 2.2 we have that $\langle H_{\eta_1,\eta_2}, m_\lambda\rangle \lesssim a_\lambda^{5/4}$, for $\lambda = (a_\lambda, \theta_\lambda, \mathbf{p})$. Lemma 2.3 then says that it follows $\langle \chi_\mathcal{R}, m_\lambda\rangle \lesssim a_\lambda^{5/4}$, where with $\mathcal{R}$ we denote the locally linear (around $\mathbf{p}$) approximation of Ω. Since Lemma 2.4 tells us that $\langle \chi_\Omega - \chi_\mathcal{R}, m_\lambda\rangle \leqslant a_\lambda^{C_N}$, where $C_N > \frac{5}{4}$ provided $\hat{m}_\lambda$ is sufficiently smooth, it follows by equation (33) that $\langle \chi_\Omega, m_\lambda\rangle \lesssim a_\lambda^{5/4}$, where the higher order terms can be readily neglected. Analogous analysis gives that $\langle \chi_\Omega, m_\lambda\rangle \lesssim a_\lambda^{3/4}$ holds when θ_λ is orthogonal to either η_1 or η_2. □

5 Multiplication with a Smooth Function

Theorem 4.11 admits a very simple and immediate generalisation.In the following we will try to address the decay rates for coefficients of the form $\langle f\chi_\Omega, m_\lambda\rangle$, where f is a (locally) smooth function. To begin the analysis we will look at monomials and build up from

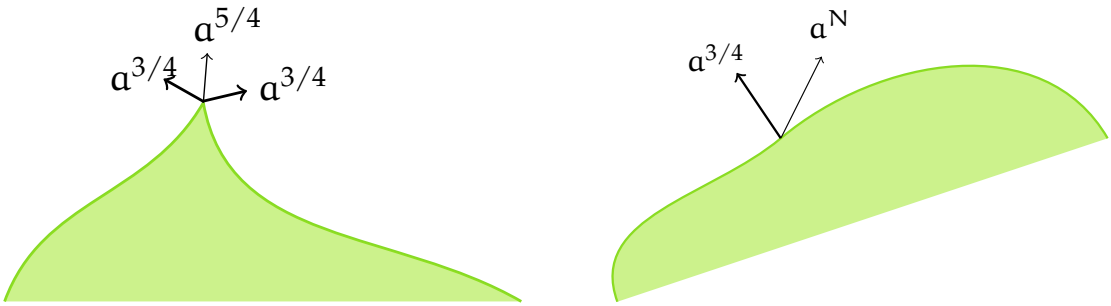

(a) Decay rates at a corner point. The rates $a^{3/4}$ correspond to orthogonal directions while $a^{5/4}$ correspond to the non-orthongal directions

(b) On smooth parts of the boundary we have the decay rate $a^{3/4}$ in the orthogonal direction and otherwise a^{N}

Figure 3: Decay rates of the points along the edge of a domain.

there. For a multi-index $\boldsymbol{\alpha} \in \mathbb{N}_0^2$ we compute

$$\langle \mathbf{x}^{\boldsymbol{\alpha}} \chi_\Omega, m_\lambda \rangle = \langle \chi_\Omega, \mathbf{x}^{\boldsymbol{\alpha}} m_\lambda \rangle = C_{\boldsymbol{\alpha}} \langle \hat{\chi}_\Omega, \partial^{\boldsymbol{\alpha}} (\hat{m}_\lambda) \rangle = C_{\boldsymbol{\alpha}} \left\langle \hat{\chi}_\Omega, \sum_{|\boldsymbol{\beta}|=|\boldsymbol{\alpha}|} C_{\theta,\boldsymbol{\beta}} a_\lambda^{\beta_1 + \frac{\beta_2}{2}} \hat{m}_{\lambda,\boldsymbol{\beta}} \right\rangle$$

$$= C_{\boldsymbol{\alpha}} \sum_{|\boldsymbol{\beta}|=|\boldsymbol{\alpha}|} C_{\theta,\boldsymbol{\beta}} a_\lambda^{\beta_1 + \frac{\beta_2}{2}} \langle \hat{\chi}_\Omega, \hat{m}_{\lambda,\boldsymbol{\beta}} \rangle, \tag{34}$$

where

$$\hat{m}_{\lambda,\boldsymbol{\beta}} = a_\lambda^{3/4} \varphi_{\boldsymbol{\beta}}^{(\lambda)} \left(D_{a_\lambda} R_{\theta_\lambda} \xi \right) \text{ and } \varphi_{\boldsymbol{\beta}}^{(\lambda)}(\xi) = \partial^{\boldsymbol{\beta}} \varphi^{(\lambda)}(\xi). \tag{35}$$

Extracting the highest common power of the dilation parameter from the expression (34), we have

$$\langle \mathbf{x}^{\boldsymbol{\alpha}} \chi_\Omega, m_\lambda \rangle \lesssim a_\lambda^{\frac{|\boldsymbol{\alpha}|}{2}} \sum_{|\boldsymbol{\beta}|=|\boldsymbol{\alpha}|} \langle \chi_\Omega, m_{\lambda,\boldsymbol{\beta}} \rangle. \tag{36}$$

The analysis developed in tpreceding sections can now be readily applied to each of the coefficients $\langle \chi_\Omega, m_{\lambda,\boldsymbol{\beta}} \rangle$. A careful examination of the arguments in previous sections reveals that the computations, and the subsequent decay rates, came about by applying the time-frequency localisation of functions m_λ to show boundedness of various integrals, that is, solely by using the decay conditions (1) and the smoothness of $\hat{m}_\lambda$. However, it is clear from (35) that the functions $m_{\lambda,\boldsymbol{\beta}}$ satisfy the decay conditions (1), provided $\hat{m}_\lambda$ is smooth enough. To be more precise, $m_{\lambda,\boldsymbol{\beta}}$ is of order $(R - |\boldsymbol{\beta}|, M, N_1, N_2)$, assuming m_λ is a molecule of order (R, M, N_1, N_2). Therefore, applying the results of Theorem 4.11, for a corner point $\mathbf{p}$ and $\lambda = (a_\lambda, \theta_\lambda, \mathbf{p})$, we have

$$\langle \mathbf{x}^{\boldsymbol{\alpha}} \chi_\Omega, m_\lambda \rangle \lesssim a_\lambda^{5/4 + \frac{|\boldsymbol{\alpha}|}{2}},$$

when m_λ is not orthogonal to the tangents at $\mathbf{p}$ and

$$\langle \mathbf{x}^{\boldsymbol{\alpha}} \chi_\Omega, m_\lambda \rangle \lesssim a_\lambda^{3/4 + \frac{|\boldsymbol{\alpha}|}{2}},$$

when it is.

The same line of argument can now be extended to general polynomials. Consider a polynomial $P_{\boldsymbol{\alpha}}(\mathbf{x})$, of finite degree, such that $\partial^{\boldsymbol{\beta}} P_{\boldsymbol{\alpha}}(\mathbf{0}) = 0$, for all multi-indices $\boldsymbol{\beta} \in \mathbb{N}_0^2$ such that$|\boldsymbol{\beta}| \leqslant \boldsymbol{\alpha}$, where $\boldsymbol{\alpha}$ is the smallest element of $\mathbb{N}_0^2$ with that property. In other words, $P_{\boldsymbol{\alpha}}$ satisfies

$$P_{\boldsymbol{\alpha}}(\mathbf{x}) = \sum_{\boldsymbol{\beta} \in \mathbb{J}} C_{\boldsymbol{\beta}} \mathbf{x}^{\boldsymbol{\beta}}.$$

where $\mathbb{J} \subseteq \mathbb{N}_0^2$, with $0 < |\mathbb{J}| < \infty$, and $\boldsymbol{\alpha} = (\alpha_1, \alpha_2) \in \mathbb{N}_0^2$ is defined by $\alpha_i = \min_{\boldsymbol{\beta} \in \mathbb{I}} \beta_i$, for $i = 1, 2$. If $\mathbf{p}$ is a corner point of Ω it follows by linearity

$$\begin{aligned}\langle P_{\boldsymbol{\alpha}} \chi_\Omega, m_\lambda \rangle &= \sum_{\boldsymbol{\beta} \in \mathbb{J}} C_{\boldsymbol{\beta}} \langle \mathbf{x}^{\boldsymbol{\beta}} H_{\eta_1, \eta_2}, m_\lambda \rangle \lesssim a_\lambda^{\frac{|\boldsymbol{\alpha}|}{2}} \sum_{\boldsymbol{\beta} \in \mathbb{J}} \sum_{|\boldsymbol{\gamma}| = |\boldsymbol{\beta}|} \langle \chi_\Omega, m_{\lambda, \boldsymbol{\gamma}} \rangle \\ &\lesssim a_\lambda^{5/4 + \frac{|\boldsymbol{\alpha}|}{2}}, \end{aligned} \tag{37}$$

when the molecule m_λ is not orthogonal to $\partial\Omega$ at $\mathbf{p}$. An analogous argument shows that $\langle P_{\boldsymbol{\alpha}} \chi_\Omega, m_\lambda \rangle \lesssim a_\lambda^{3/4 + \frac{|\boldsymbol{\alpha}|}{2}}$ when m_λ is not orthogonal to $\partial\Omega$ at $\mathbf{p}$.

Remark. It would be possible to produce a more precise assessment of the decay rates had we picked the underlying parabolic molecule with more scrutiny. To argue that this is the case it is sufficient to re-examine (34). The fundamental issue that hinders a better analysis lies in the fact that a general parabolic molecule $\hat{m}_\lambda$ does not separate ξ_1 and ξ_2. Consequently, any partial derivative of $\hat{m}_\lambda$ will necessarily involve all partial derivatives of the same order and the dilations imposed by the matrix D_a cannot be decoupled. A much finer analysis could be obtained by considering parabolic families that can achieve this decoupling, such as the classical shearlets [6, 16]. We shall not pursue this line of argument since imposing such restrictions would be at odds with what we are trying to achieve. Interested reader is directed to [18] for a further discussion on this topic.

We can now extend our analysis to more general functions by locally approximating a given function with its Taylor polynomial. Take $f \in C^m(\mathbb{R}^2)$ and denote by P_k its Taylor polynomial of degree k around $\mathbf{p}$, that is

$$f(\mathbf{x}) = \sum_{|\boldsymbol{\alpha}| \leqslant k} \partial^{\boldsymbol{\alpha}} f(\mathbf{p}) (\mathbf{x} - \mathbf{p})^{\boldsymbol{\alpha}} + R_k(\mathbf{x}) = P_k(\mathbf{x}) + R_k(\mathbf{x}). \tag{38}$$

Let $\mathbf{p}$ be a corner point of Ω and assume without loss of generality that $\mathbf{p} = \mathbf{0}$. Let f be such that $\partial^{\boldsymbol{\beta}} f(\mathbf{0}) = 0$, holds for all $\boldsymbol{\beta} \in \mathbb{N}_0^2$ such that $|\boldsymbol{\beta}| \leqslant l$, where $l < k$. Then it follows

$$\langle f \chi_\Omega, m_\lambda \rangle = \langle f \chi_\Omega - P_k \chi_\Omega, m_\lambda \rangle + \langle P_k \chi_\Omega, m_\lambda \rangle. \tag{39}$$

Therefore, provided

$$\langle f \chi_\Omega - P_k \chi_\Omega, m_\lambda \rangle \lesssim a_\lambda^N, \tag{40}$$

holds for a big enough $N \in \mathbb{N}$, it will follow

$$\langle f \chi_\Omega, m_\lambda \rangle \lesssim a_\lambda^{q + \frac{|\boldsymbol{\alpha}|}{2}}, \tag{41}$$

where $q = \frac{3}{4}$ when m_λ is orthogonal to $\partial\Omega$ at $\mathbf{p}$, and $q = \frac{5}{4}$ otherwise.

The proof of (40) is analogous to that of Lemma 4.10, and it is the content of Lemma A.1 which can be found in the Appendix. Furthermore, (41) clearly holds not just for globally smooth functions but for more general classes of functions by adhering to the localisation Lemma 4.1.

Looking at (41) we see that the resulting rate of decay comes from two contributions. The factor a^q. for $q = 3/4$ or $q = 5/4$, comes from coefficients of the form $\langle \chi_\Omega, \varphi_\lambda \rangle$, where φ_λ is a partial derivative of a CPM and satisfies a condition of the form (1). The second contribution, $a^{\frac{|\boldsymbol{\alpha}|}{2}}$, comes by using the property of the Fourier transform to draw a relationship between polynomial multiplication in the space domain with partial derivatives in the frequency domain. In other words, if a corner point $\mathbf{p}$ is a root of f, then the strength of singularity of $f\chi_\Omega$ at $\mathbf{p}$ is counteracted by the multiplicity of the root, and this can be observed through the increased rate of decay of the frame coefficients. The rate of decay will increase relative to the multiplicity of the root.

We can now use the approximation strategy developed in Section 4.5 to extended the results for any set Ω satisfying the assumptions of Theorem 4.11.

Theorem 5.1. *Let $f \in C^m(\mathbb{R}^2)$ be a function such that $\partial^\beta f(\mathbf{p}) = 0$, for all $\beta \in \mathbb{N}_0^2$ such that $|\beta| \leqslant l$, and let $P_k(\mathbf{x})$ be its corresponding Taylor polynomial around $\mathbf{p}$ of degree k where $k > l$. Assume a family of continuous parabolic molecule $\Gamma = \{m_\lambda : \lambda \in \Lambda_\Gamma\}$ and a set Ω satisfy the conditions of Theorem 4.11. Consider a corner point $\mathbf{p}$ of Ω, and take $\lambda = (a_\lambda, \theta_\lambda, \mathbf{p})$. If θ_λ is orthogonal to neither $\alpha'_\Omega(t_0^+)$ nor $\alpha'_\Omega(t_0^-)$, where $\alpha_\Omega(t_0) = \mathbf{p}$ then*

$$\langle f\chi_\Omega, m_\lambda \rangle \lesssim a_\lambda^{5/4+\frac{|\alpha|}{2}},$$

and otherwise

$$\langle f\chi_\Omega, m_\lambda \rangle \lesssim a_\lambda^{3/4+\frac{|\alpha|}{2}}.$$

Proof. Consider (39), and estimate the first term by (40) using Lemma A.1. The statement then follows by (37). □

6 α-Molecules

Throughout the preceding analysis we used the parabolic scaling of the variables, as dictated by Definition 2.1. A natural question is how, and indeed if, would the results change if we chose a different scaling law. Since the parabolic scaling is propagated through the parabolic dilation matrices, the most immediate work-around would be to generalise the dilation matrices by $D_{a,\alpha} = \mathrm{diag}(a, a^\alpha)$ where $\alpha \in [0, 1]$, and revise the definition of continuous molecules accordingly. Constructions of this type are typically called *α-molecules* [21]. Notice that the parabolic molecules correspond to the case $\alpha = 1/2$.

We will not be concerned at this point with questions regarding existence or the convergence of integrals and such things, but rather just with quantitative changes in terms of the decay with respect to the scaling parameter a. It follows immediately that $a^{5/4}$ ought to be replaced with $a^{\frac{3-\alpha}{2}}$, and $a^{3/4}$ with $a^{\frac{1+\alpha}{2}}$, in e.g. statements of Theorems 4.6 and 4.7. Therefore, taking $\alpha = 1$ (which corresponds to the case when we treat both axes equally and the isotropic directional wavelets) we get that the decay rates satisfy $\frac{3-\alpha}{2} = \frac{1+\alpha}{2}$. Therefore, we cannot distinguish between edge and corner points, nor can we distinguish between different orientations associated to a corner point. This means that that we indeed need an unequal treatment of the axes to conduct analysis of this type.

Furthermore, changing the dilation matrices does not change the conditions of Lemma 2.4, that is, in order for the lemma to hold we again get the conditions

$$-\frac{1+\alpha}{2} + \gamma(k+1) > \frac{3-\alpha}{2}, \quad \text{and} \quad 2N(1-\gamma) - \frac{1+\alpha}{2} + \gamma > \frac{3-\gamma}{2},$$

which are readily reduced to $\gamma > \frac{2}{k+1}$, and $\gamma < 1 - \frac{1}{2N-1}$. But, those are exactly the same conditions we got with parabolic molecules. Therefore, the conclusion would remain the same, which means that from the theoretical perspective, when it comes to the detection of geometric features such as corner points, the particular choice of a scaling law does not make a tangible effect as long as some sort of directional bias is present.

7 A Look at Earlier Work and a Simple Numerical Test

As we have mentioned on more than one occasion, the main contribution of our work is the level of generality. This generality comes with the obvious drawbacks and we make no claims with regards to the real-world applicability. We will now put the results presented here in the context of contemporary research. Apart from the initial studies in [5] and [15], we are aware of two approaches that are currently on the market. The common feature across the existing methods is a two step process that combines an approximation procedure and a localisation argument to yield results on edge and corner detection.

The first approach, studied for example in [16] and [3], relies on a couple of features. Firstly, the underlying dictionary is assumed (or rather constructed) to be band-limited, where the mother function separates the angular and radial influences in one way or another. The next step uses an ingenious trick, taken from [22] and [23] to compute the Fourier transform of χ_Ω. Let $\Omega \subseteq \mathbb{R}^2$ again be an open and bounded set whose parametrisation is denoted by α_Ω and define

$$F(\xi, x) = (F_1(\xi, x), F_2(\xi, x)) = -2\pi\imath\|\xi\|^{-2} e^{-2\pi\imath\xi\cdot x}\xi^\perp, \text{ where } \xi^\perp = (-\xi_2, \xi_1)^\top.$$

Using the Green's theorem (or the divergence theorem) we then have

$$\begin{aligned}\hat{\chi}_\Omega(\xi) &= \int_\Omega e^{2\pi\imath\xi\cdot x} dx = \int_\Omega \left(\partial^{(1,0)} F_2(\xi, x) - \partial^{(0,1)} F_1(\xi, x)\right) dx \\ &= \int_{\partial\Omega} F(\xi, \alpha_\Omega(t))\alpha_\Omega'(t) dt \\ &= -\frac{1}{2\pi\imath\|\xi\|^2} \int_{\partial\Omega} e^{-2\pi\imath\xi\cdot\alpha_\Omega(t)} \xi^\perp \cdot \alpha_\Omega'(t) dt\end{aligned}$$

The phase $\xi \cdot \alpha_\Omega(t)$ becomes stationary when $\xi \cdot \alpha_\Omega'(t) = 0$, which corresponds to the case when ξ is normal to the boundary curve. Going to polar coordinates, one then studies the behaviour of $\hat{\chi}_\Omega$ as $\|\xi\|$ tends to infinity and uses the method of stationary phase. Studying the coefficients $\langle \hat{\chi}_\Omega, m_\lambda \rangle$ with respect to a band-limited family of functions allows one to precisely isolate the orientations of the normals at edge and corner points.

The second approach, observed in [17], studies the case when the underlying dictionary is compactly supported. This assumption poses a unique set of challenges since a limited smoothness in the spatial domain gives a comparatively limited decay in the frequency domain, but this study is grounded in the understanding that the singularities of two-dimensional objects are essentially local properties in the spatial domain. Hence, the computations are conducted in the spatial domain, using so-called *detector shearlets*. The results are promising and some aspects of their functionality can be extended to three dimensions.

The results in [16], [17], and our results agree in several respects. In all three studies, frame coefficients at an edge point admit the decay rate of $a^{3/4}$ when the molecule is orthogonal to $\partial\Omega$ at a given point, and the rate a^N holds in all other directions. These results are in accordance with earlier studies in [16] and [3]. Furthermore, the decay rates for a corner point $\mathbf{p}$, when the molecule is orthogonal to $\partial\Omega$ at $\mathbf{p}$, are in all three cases $a^{3/4}$. Where the results differ is the case when the given molecule is not orthogonal to $\partial\Omega$ at a corner point. The results in [17] and our results suggest that the rate is $a^{5/4}$ whereas the results of [16] suggest the rate $a^{9/4}$, which is claimed to be the result of cancellations of certain integrals which is attributed to the properties of the underlying shearlet family. Notice that this is not an immediate contradiction with our results since we claim only upper bounds.

The follow-up studies to those [16] can be found in [18], where the authors conducted studies similar to those in Section 5, as we previously indicated. In [18] the authors use a somewhat unorthodox construction of shearlets where the mother shearlet is defined by

$$\hat{\psi}(\xi) = w(\xi_1)v\left(\frac{\xi_2}{\xi_1}\right), \quad \text{where } \operatorname{supp} w, \operatorname{supp} v \subseteq [-1, 1].$$

Therefore, the mother shearlet is a classical shearlet (cf. Chapter 1 in [6]) but its support is non-standard since the support of w is centred around the origin, whereas the standard construction obeys

$$\hat{\psi}(\xi) = \psi_1(\xi_1)\psi_2\left(\frac{\xi_2}{\xi_1}\right), \text{ where } \operatorname{supp}\hat{\psi}_1 \subseteq \left[-2, -\frac{1}{2}\right] \cup \left[\frac{1}{2}, 2\right] \text{ and } \operatorname{supp}\hat{\psi}_2 \subseteq [-1, 1]. \tag{42}$$

The results that follow are analogous to those in the earlier paper [16], and it is claimed that cancellations of the same type still occur, including the case of coefficients of the form $\langle f\chi_\Omega, \psi_\lambda\rangle$.

Due to this unorthodox nature of the underlying shearlet constructions, its disagreement with other work, and a couple of other peculiarities that a diligent examination of the proofs seems to uncover, we decided to conduct a very simple numerical study of the asymptotics of decay rates for shearlets constructed in the initial paper [16], since the work in [18] is based on those results. To conduct this small experiment we used MATLAB to compute the values of the coefficients $\langle H_{\eta_1,\eta_2}, m_\lambda\rangle$, for $\theta_\lambda = 0$ and a various selection of η_1 and η_2 which correspond to the case when the molecule is not orthogonal to the wedge $\mathcal{W}_{\eta_1,\eta_2}$ at $\mathbf{p} = \mathbf{0}$, and the range of dilations $a = 2^{-5}, \ldots, 2^{-10}$. We then computed the extrapolated decay rates.

The chosen family of shearlets was such that it satisfies the assumptions of the initial work in [16], where the authors considered a mother shearlet obeying the classical construction (42), and where $\hat{\psi}_1$ is a smooth and odd function, and $\hat{\psi}_2$ is an even function that decreases on $[0, 1)$ and obeys $\|\psi_2\|_2 = 1$. The results are summarised in Table 1.

	$\eta_1 = \pi/6$	$\eta_1 = 2\pi/6$	$\eta_1 = \pi/30$	$\eta_1 = -\pi/6$
Angles	$\eta_2 = 5\pi/6$	$\eta_2 = 7\pi/6$	$\eta_2 = 2\pi/6$	$\eta_2 = 3\pi/6$
Extrapolated Rates	1.2504	1.2557	1.2542	1.2536

Table 1: Extrapolated decay rates of frame coefficients

Our elementary numerical study seems to confirm that the rate $a^{5/4}$ is the actual rate in this context. We make no claims regarding the robustness, or the conclusiveness of our numerical experiment and its results, for which a more detailed study would be needed, rather it is merely meant as an indication. We should add that we believe the results in [16] and [18] are still essentially valid, though perhaps with some minor tweaks.

8 Concluding Remarks

In this paper we presented arguments that provide upper bounds on the decay rate of frame coefficients at corner points. While it might be possible to produce lower bounds as well, this does not seem likely since the existing results on upper bounds hold only in very specific cases, that is, only for delicately constructed families of shearlets; look at the discussion in [17, 16]. Therefore, because our approach is based in generality and the level of abstractness, lower bounds seem out of reach. On the other hand, it might be possible to get a microlocal characterisation of corner points by perhaps using the geometrical dependence of the angle at the corner point and the orientation parameter of the molecule.

Another topic of interest is the analysis of corner points of the j^{th} order, that is, instead of considering only $\alpha'(t_0^+) \neq \alpha'(t_0^-)$, we could look at $\alpha^{(j)}(t_0^+) \neq \pm\alpha^{(j)}(t_0^-)$. Our approach cannot be directly adapted to these cases on account of the fact that there is a direct correlation between the smoothness of the boundary around a given point, and the decay rates of coefficients with a given directional parabolic frame; the higher the smoothness the faster the decay with respect to the dilation parameter. On the other hand, since the nature of our approach means that we are assessing the approximation rather than assessing the set itself, higher decay rates are rendered undetectable due to the fact that we are using a first order approximation. Thus, a different approach would be required. Furthermore, it would be desirable to know the dependence of the decay rates with respect to other geometrical features of the boundary curve, such as its curvature. At the moment there are some results for band-limited molecules, but thus far they are not in

the generality we would want them to be.

A Appendix

Lemma A.1. *Let $f \in C^m$ and let $P_k(\mathbf{x})$ be its corresponding Taylor polynomial around $\mathbf{p}$ of degree k where $k > l$. Assume that $\Gamma = \{m_\lambda : \lambda \in \Lambda_\Gamma\}$ is a family of continuous parabolic molecules of high-enough order and that Ω is a set that satisfies the conditions of Theorem 4.11. Then*

$$\langle f\chi_\Omega - P_{\boldsymbol{\alpha}}\chi_\Omega, m_\lambda\rangle \lesssim a_\lambda^K, \tag{43}$$

holds for $K > \frac{5}{4}$.

Proof. Without loss of generality let us assume $\mathbf{p} = \mathbf{0}$ and drop the λ indices. We have

$$\begin{aligned}|\langle f\chi_\Omega - P_k\chi_\Omega, m\rangle| &\leqslant \int_{\mathbb{R}^2} |f(\mathbf{x}) - P_k(\mathbf{x})||\chi_\Omega(\mathbf{x})||m_\lambda(\mathbf{x})|d\mathbf{x} \\ &= \underbrace{\int_{\mathcal{B}_{a^\gamma}(\mathbf{0})} |f(\mathbf{x}) - P_k(\mathbf{x})||\chi_\Omega(\mathbf{x})||m(\mathbf{x})|d\mathbf{x}}_{I_1} \\ &\qquad + \underbrace{\int_{\mathcal{B}^c_{a^\gamma}(\mathbf{0})} |f(\mathbf{x}) - P_k(\mathbf{x})||\chi_\Omega(\mathbf{x})||m(\mathbf{x})|d\mathbf{x}}_{I_2}.\end{aligned}$$

Estimating I_1 gives

$$\begin{aligned}I_1 &= \int_{\mathcal{B}_{a^\gamma}(\mathbf{0})} |f(\mathbf{x}) - P_k(\mathbf{x})||\chi_\Omega(\mathbf{x})||m(\mathbf{x})|d\mathbf{x} \lesssim a^{-3/4}\int_{\mathcal{B}_{a^\gamma}(\mathbf{0})} |f(\mathbf{x}) - P_k(\mathbf{x})||\chi_\Omega(\mathbf{x})|d\mathbf{x} \\ &\lesssim \int_{\mathcal{B}_{a^\gamma}(\mathbf{0})} |\mathbf{x}|^k d\mathbf{x} \lesssim a^{\gamma(k+2)},\end{aligned}$$

where $\gamma > 0$. On the other hand, for I_2 we have

$$\begin{aligned}I_2 &= \int_{\mathcal{B}^c_{a^\gamma}(\mathbf{0})} |f(\mathbf{x}) - P_k(\mathbf{x})||\chi_\Omega(\mathbf{x})||m(\mathbf{x})|d\mathbf{x} \lesssim \int_{\mathcal{B}^c_{a^\gamma}(\mathbf{0})} |\varphi(\mathbf{x})|\, d\mathbf{x} \\ &\lesssim \int_{\mathcal{B}^c_{a^\gamma}(\mathbf{0})} \left(1 + a^{-2}x_1^2 + a^{-1}x_2^2\right)^{-N} d\mathbf{x} \lesssim a^{N-3/4}\int_{a^\gamma}^\infty r^{-1-2N} dr \lesssim a^{N(1-2\gamma)-3/4}\end{aligned}$$

Therefore, the statement holds for $0 < \gamma < \frac{1}{2}$ such that and $\gamma(k+2) > \frac{5}{4}$ and provided N is big enough. □

References

[1] A. Gelb and D. Cates. Segmentation of Images from Fourier Spectral Data. *Commun. Comput. Phys.*, 5(2-4):326–349, 2009.

[2] T. A. Gallagher, A. J. Nemeth, and L. Hacein-Bey. An Introduction to the Fourier Transform: Relationship to MRI. *Amer. J. of Roentgen.*, 180(5):1396–1405, 2008.

[3] L. Greengard and C. Stucchio. Spectral Edge Detection in Two Dimensions Using Wavefronts. *Appl. Comput. Harmon. Anal.*, 30:69–95, 2011.

[4] D. L. Donoho. Sparse Components of Images and Optimal Atomic Decompositions. *Constr. Approx.*, 17(3):353–382, 2001.

[5] E. J. Candès and D. L. Donoho. Continuous Curvelet Transform: I. Resolution of the Wavefront Set. *Appl. Comput. Harmon. Anal.*, 19:162–197, 2003.

[6] G. Kutyniok, D. Labate, and Editors. *Shearlets: Multiscale Analysis for Multivariate Data*. Birkhäuser, 2012.

[7] M. N. Do and M. Vetterli. The Contourlet Transform: an Efficient Directional Multiresolution Image Representation. *IEEE Trans. Image Process.*, 14(12):2091–2106, 2015.

[8] C. Durasanti, J. D. McEwen, and Y. Wiaux. Localisation of Directional Scale-Discretised Wavelets on the Sphere. *Appl. Comput. Harmon. Anal.*, 2016.

[9] G. Hennenfent and F. J. Herrmann. Seismic Denoising with Nonuniformly Sampled Curvelets. *IEEE Comput. Sci. Eng.*, 8(3):906–916, 2006.

[10] E. J. Candès, D. L. Donoho, and J-L. Starck. The Curvelet Transform for Image Denoising. *IEEE Trans. Image Process.*, 11(6):131–141, 2002.

[11] E. J. Candès and L. Demanet. The Curvelet Representation of Wave Propagators is Optimally Sparse. *Comm. Pure Appl. Math.*, 58:1472–1528, 2004.

[12] P. Grohs and G. Kutyniok. Parabolic Molecules. *Found. Comput. Math.*, pages 299–337, 2013.

[13] P. Grohs and Z. Kereta. Continuous Parabolic Molecules. Technical report, SAM ETHZ, 2015.

[14] E. J. Candès and D. L. Donoho. New Tight Frames of Curvelets and Optimal Representations of Objects with Piecewise C^2 Singularities. *Comm. Pure Appl. Math.*, 57(2):219–266, 2004.

[15] G. Kutyniok and D. Labate. Resolution of the Wavefront Set Using Continuous Shearlets. *Trans. Amer. Math. Soc.*, 361(5):2719–2754, 2009.

[16] K. Guo and D. Labate. Characterization and Analysis of Edges Using the Continuous Shearlet Transform. *SIAM J. Imaging Sci.*, 2(3):959–986, 2009.

[17] G. Kutyniok and P. Petersen. Classification of Edges Using Compactly Supported Shearlets. *Appl. Comput. Harmon. Anal.*, 2015.

[18] K. Guo and D. Labate. Characterization and Analysis of Edges in Piecewise Smooth Functions. *Appl. Comput. Harmon. Anal.*, 2015.

[19] H. F. Smith. A Parametrix Construction for Wave Equations with $C^{1,1}$ Coefficients. *Ann. de l'Institut Fourier*, pages 797–835, 1998.

[20] M. E. Taylor. *Pseudodifferential Operators*. Princeton University Press, 1981.

[21] P. Grohs, G. Kutyniok, S. Keiper, and M. Schäfer. α-molecules. *Appl. Comput. Harmon. Anal*, 42:297–336, 2016.

[22] C. S. Herz. Fourier Transforms Related to Convex Sets. *Ann. of Math.*, 2(75):81–92, 1962.

[23] E. Sorets. Fast Fourier Transforms of Piecewise Constant Functions. *J. Comp. Phys.*, 116(2):395–379, 1995.

[24] T. Tao. Lecture Notes for Fourier Analysis at UCLA. http://www.math.ucla.edu/ tao/247a.1.06f/notes2.pdf.

[25] H. F. Smith. A Hardy Space for Fourier Integral Operators. *J. Geom. Anal.*, 8(4):629–653, 1998.

[26] K. Guo and D. Labate. Optimally Sparse Multidimensional Representation using Shearlets. *SIAM J. Math. Anal.*, 39:298–318, 2007.

[27] G. Kutyniok and D. Labate. The Construction of Regular and Irregular Shearlet Frames. *J. Wavelet Theory Appl.*, 1:1–10, 2007.

[28] C. D. Sogge. *Fourier Integrals in Classical Analysis*. Cambridge University Press, 1993.

[29] A. Grigis and J. Sj. *Microlocal Analysis for Differential Operators: An Introduction*. Cambridge University Press, 1994.

[30] R. B. Melrose and G. Uhlmann. An Introduction to Microlocal Analysis. http://www-math.mit.edu/ rbm/books/imaast.pdf, 2000.

[31] E. J. Candès and D. L. Donoho. Continuous Curvelet Transform: Ii. Discretization and Frames. *Appl. Comput. Harmon. Anal*, 19:198–222, 2003.

[32] R. S. Strichartz. *A Guide to Distribution Theory and Fourier Transforms*. World Scientific, 2003.

[33] S. Mallat. *A Wavelet Tour of Signal Processing*. Academic Press, third edition, 2009.

[34] I. M. Gelfand and G. E. Shilov. *Generalized Functions: Volume I - II*. Academic Press, 1964.

[35] L. Hörmander. *The Analysis of Linear Partial Differential Operators I*. Springer, second edition, 1990.

[36] E. J. King, G. Kutyniok, and X. Zhuang. Analysis of Inpainting via Clustered Sparsity and Microlocal Analysis. *J. Math. Imaging Vision*, 48:205–234, 2014.

[37] C. Brouder, N. V. Dang, and F. Helein. A Smooth Introduction to the Wavefront Set. http://arxiv.org/abs/1404.1778, 2014.

[38] S. Mallat and G. Peyré. A Review of Bandlet Methods for Geometrical Image Representation. *Numer. Algorithms*, 44(3):205–234, 2007.

[39] E. J. Candès and D. L. Donoho. Curvelets and Curvilinear Integrals. *J. Approx. Theory*, 113(1):59–90, 2001.

[40] J. Fadili and J-L. Starck. Curvelets and Ridgelets, 2007.

[41] I. Daubechies, A. Grossman, and Y. Meyer. Painless Nonorthogonal Expansions. *J. Math. Phys.*, 27(5):1271–1283, 1986.

[42] P. Grohs. Continuous Shearlet Frames and Resolution of the Wavefront Set. *Monatsh. Math.*, 164:393–426, 2010.